AN ABSTRACT OF THE THESIS OF

Matthew M. Cox for the degree of Master of Science in Bioresource Engineering presented on April 8, 2002

Title: A Spatially Explicit Network-Based Model for Estimating Stream Temperature Distribution

Redacted for privacy

Abstract approved: _____
John P. Bolte

The WET-Temp (Watershed Evaluation Tool – Temperature) model is designed to take advantage of spatially explicit datasets to predict stream temperature distribution. Datasets describing vegetation cover, stream network locations, elevation and stream discharge are utilized by WET-Temp to quantify geometric relationships between the sun, stream channel and riparian areas. These relationships are used to estimate the energy gained or lost by the stream via various heat flux processes (solar and longwave radiation, evaporation, convection and advection). The sum of these processes is expressed as a differential energy balance equation applied at discrete locations across the stream network. The model describes diurnal temperature dynamics at each of these locations and thus temperature distribution across the entire network. WET-Temp is calibrated to a tributary of the South Santiam River in western Oregon, McDowell Creek. The mean differences between measured and modeled values in McDowell Creek were 0.6°C for daily maximum temperature and 1.3°C for daily minimum temperature. The model was then used to predict maximum and minimum temperatures in an adjacent tributary, Hamilton Creek. The mean differences between modeled and measured values in this paired basin were 1.8°C for daily maximum temperatures and 1.4°C for daily minimum temperatures. Influences of model parameters on modeled temperature distributions are explored in a sensitivity analysis. The ability of WET-Temp to utilize spatially explicit datasets in estimating temperature distributions across stream networks advances the state of the art in modeling stream temperature.

A Spatially Explicit Network-Based Model for Estimating Stream Temperature Distribution

by
Matthew M. Cox

A THESIS

submitted to

Oregon State University

in partial fulfillment of
the requirements for the
degree of

Master of Science

presented April 8, 2002
commencement June 2003

Master of Science thesis of Matthew M. Cox presented on April 8, 2002

APPROVED:

Redacted for privacy

Major Professor, representing Bioresource Engineering

Redacted for privacy

Head of the Department of Bioengineering

Redacted for privacy

Dean of the Graduate School

I understand that my thesis will become part of the permanent collection of Oregon State University libraries. My signature below authorizes release of my thesis to any reader upon request

Redacted for privacy

Matthew M. Cox, Author

ACKNOWLEDGEMENTS

I would like to extend my sincere appreciation to Dr. John Bolte for his constant availability, and his assistance in the navigation of a programming sea where I knew few landmarks. Additionally, the comments of Dr. Jim Moore, Dr. Sherri Johnson and Dr. Robert Beschta were formative in my appreciation of the complexities of temperature in streams. A special thanks is in order for Kellie Vache, who answered countless questions on countless subjects between the office and the coffee shop.

This project has been greatly assisted by the Oregon Department of Environmental Quality. Thanks go out to Agnes Lut and others at DEQ who shared their data and expertise.

TABLE OF CONTENTS

TABLE OF CONTENTS (CONTINUED)

TABLE OF CONTENTS (CONTINUED)

LIST OF FIGURES

LIST OF TABLES

LIST OF APPENDIX FIGURES

LIST OF APPENDIX TABLES

A Spatially Explicit Network-based Model for Estimating Stream Temperature Distribution

Introduction

Watershed councils are groups of landowners and residents coming together in an attempt to improve the quality of their watershed. These groups are voluntary, have no regulatory powers, and are locally organized (Oregon Watershed Enhancement Board, 2000). These groups have access to funding used for restoration projects. The councils must make decisions on project size and location, and must prioritize projects under limited budgets.

Watershed councils make some very important decisions, but may have limited access to technical expertise regarding ecosystem function and the planning of restoration strategies. The RESTORE model was developed in response to this need. It is a tool created to assist councils in evaluating the potential ecological and economic outcomes of restoration strategies at the watershed scale. RESTORE is designed to take advantage of watershed scale hydrologic and ecological models as well as economic valuation of restoration strategies. These models are applied with stakeholder-determined constraints to represent the collective goals and values of the council (Oregon State University Biosystems Analysis Group, 1998).

RESTORE generates potential landscapes given restoration strategies that represent a watershed council's collective interests. After these landscapes are generated, the next step is the evaluation of the affect of these potential strategies on various ecological goals (increased habitat for pond turtles, decreased sediment loads etc...). Evaluative models are being created to examine these affects. WET-Temp (Watershed Evaluation Tool – Temperature) is intended to examine the potential outcomes of restoration strategies focused on the amelioration of

anthropogenic stream warming. This is a timely issue because the state of Oregon will soon begin regulating solar radiation loading caused by human activities as a pollutant, and streams exceeding the current temperature standard of 64 °F (17.7 °C) for over seven days are listed as water quality limited by the Oregon Department of Environmental Quality.

As the knowledge base concerning stream habitat and water quality has grown, the connectivity in these systems has become apparent. Watershed scale studies are becoming increasingly important, and the technology to perform these studies is advancing rapidly. Spatially explicit data is becoming more widely available and increasingly detailed. The lack of a network based stream temperature model that takes advantage of spatially explicit data is addressed by the creation of WET-Temp.

WET-Temp will allow users to evaluate the effects of potential restoration strategies on their temperature goals. It will also be helpful, used in conjunction with RESTORE, in determining the landscape changes needed to address specific temperature issues. This knowledge can be used to guide funding allotments for watershed councils and other groups. The construction of reasonable time lines for accomplishing watershed scale stream temperature goals is then possible, given the particular group's vision and means.

A Spatially Explicit Network-based Model for Estimating Stream Temperature Distribution – Model Description

Abstract

The WET-Temp (Watershed Evaluation Tool – Temperature) model is designed to take advantage of spatially distributed datasets to predict stream temperature distributions in a basin. Datasets describing vegetation, stream network, elevation and flow are utilized by WET-Temp to describe geometric relationships between the sun, stream channel and riparian areas. These relationships are used to estimate the energy gained or lost by the stream via various heat flux processes (solar and longwave radiation, evaporation, convection, conduction and advection). The descriptions of these processes are combined into a differential energy balance equation applied at discrete locations across the network. The model describes diurnal temperature dynamics at these locations and thus temperature distribution across the entire network. The ability of this model to utilize spatially explicit datasets in estimating temperature distributions across stream networks advances the state of the art in modeling stream temperature. A companion paper discusses calibration of WET-Temp and model sensitivity.

Introduction

Elevated stream temperature is one of the most pervasive water quality issues in the Pacific Northwest today. The Oregon Department of Environmental Quality lists 869 streams or stream segments as water quality limited due to elevated temperature. This is almost five times the number listed for any other water quality

parameter (Oregon Department of Environmental Quality, 1998). Anthropogenic disturbances such as removal of riparian vegetation (Beschta et al. 1987), grazing (Belsky et al. 1999), forestry (Brown and Krygeir 1970) and urbanization (LeBlanc et al. 1997, Schroeter et al. 1996) can contribute to the warming of streams.

Metabolic rates of aquatic organisms at every trophic level, including anadromous fish species, are affected by changes in water temperature regimes (Hauer and Lamberti, 1996; Horne and Goldman, 1994). Spawning, egg incubation, and survival of juvenile trout and salmonids can all be adversely affected by temperatures over 16.0° C (Wilson et al 1987). The National Marine Fisheries Service has listed many species of Pacific Northwest salmonids as threatened or endangered (National Marine Fisheries Service, 2000), making the impacts of these elevated temperatures of special interest in this region. While fluctuating ocean conditions, inadequate passage through hydroelectric dams, and over-harvest have contributed to the decline of native fish populations, habitat degradation in spawning and rearing areas is certainly a part of the problem (McIntosh 1992, NPCC 1992).

Several models exist for stream temperature prediction at the reach scale. Scaling of these models to the watershed level however, is a difficult task. Temperature at any one reach is dependent on upstream temperatures in the network. Due to the spatial extent and network connectivity of streams, it makes intuitive sense to model water quality parameters such as temperature using spatially explicit data. This project addresses the lack of a watershed-scale temperature model that incorporates these data with the creation of WET-Temp (Watershed Evaluation Tool – Temperature). WET-Temp, a network-based model designed to take advantage of spatially distributed data, predicts stream temperature distributions based on the physics of contributing heat flux processes. Energy contributions from the most important of these processes are combined with physical representations of the stream channel and surrounding vegetation to

provide estimates of diurnal temperature fluctuations within a basin. We have sought to gain understanding of stream temperature as a network phenomenon, not simply a conglomeration of temperatures at particular reaches.

The earliest computer models describing influences of physical processes on stream temperature were developed by Beschta and Weatherred (1984), and Theurer (1984). Boyd (1996) built on these to develop Heat Source, currently the state of the art reach scale temperature model. Chen (1996) developed SHADE, a model that, in conjunction with the HSPF (Hydrological Simulation Program – Fortran) model, examined stream temperature on a watershed scale. Two main gaps however, compelled us to create WET-Temp. The first is that HSPF is not completely spatially distributed, but instead uses a semi-distributed aggregation of spatial data. The second is that, with the ability to evaluate small (< 100 m stream length) scale restoration projects a priority, it is necessary to describe the stream network at a much finer resolution than is done in the SHADE/HSPF model. WET-Temp's integration of spatial information (in the form of ESRI shapefiles and grid coverages) represents a new step in the evolution of stream temperature modeling.

WET-Temp has been designed to evaluate stream temperature responses to alternative restoration scenarios. Watershed councils, intended as the primary target users, have interest in moving towards meeting regulatory temperature standards through applications of such scenarios. The model is sensitive to the regulatory requirements of the Oregon DEQ, focusing on accurate modeling of maximum daily temperature.

Data Requirements and Network Description

The vegetation information used in WET-Temp consists of land use/land cover classes derived from Landsat Thematic Mapper satellite images (Oetter et al. 2001).

Digital elevation models with 10m resolution (obtainable from the Oregon State Service Center for GIS) were utilized. SSURGO (Soil Survey Geographic Database) soils information was obtained from NRCS (Natural Resources Conservation Service, 2001).

The stream network used by WET-Temp is divided into reaches and further into subreaches, with the dividing points termed nodes and subnodes (Figure 1.1). Stream temperature distribution estimated in WET-Temp is based around a subreach energy balance. The maximum subreach length evaluated is 30m, which is consistent with the finest scale of our input vegetation information.

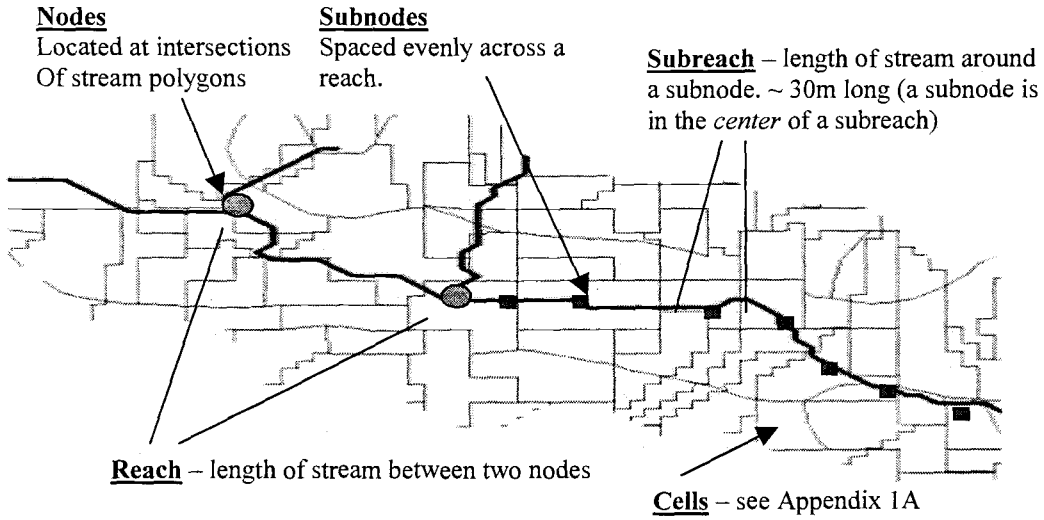

Figure 1.1 - Division of Stream Network into Reaches and Subreaches using

This model has been developed with a focus on the use of readily obtainable datasets. The following shape layers are necessary to run a WET-Temp simulation:

- Vegetation Layer - WET-Temp utilizes a 30 m grided vegetation coverage; however, any digitized vegetation information can be utilized.

- DEM Layer – 30 m grid coverage representing topography of the landscape. This layer is re-sampled from a 10 m resolution DEM to improve computational efficiency.
- Stream Layer - Representation of the stream network derived from flow accumulation calculations with a 10 m DEM.
- Flow Layer – point coverage of stream discharge observations. Only one (at the furthest reach downstream) is required, but more can be handled.
- Withdrawal Layer- point coverage describing withdrawals from the stream (optional).

Calculation of Time Invariant Parameters

The first parameters calculated are those that are unchanging with time and are associated with a specific spatial location (a node or subnode). These parameters are computed only once at the beginning of a simulation (preprocessing), and location specific information is stored for later use (see Appendix 1A).

Stream Aspect and Azimuth Angles

Knowledge of a subreach's aspect (geographic orientation) is necessary to quantify the amount of solar radiation delivered at any particular time of day. Aspect at a subnode is calculated as the angle of the vector drawn between the midpoints of the upstream and downstream subreaches, with 0 defined as due north. Two special cases must be addressed: (1) At a headwater subnode, where an upstream subreach does not exist by definition, aspect is calculated looking only downstream. (2) At a stream junction, aspect is calculated as the average aspect of the three contributing subreaches (two upstream and one downstream). The direction vectors in this case tend to average to a value similar to that of the

downstream subreach, as they are oriented in the same general downslope direction.

The first step in determining aspect is calculating the orientation angle (α) of the stream relative to north:

$$\alpha = \arctan\left[\frac{|x_2 - x_1|}{|y_2 - y_1|}\right] \qquad \text{(Eq 1.1)}$$

where,

x_1, y_1: coordinates at the start (upstream) of the subreach

x_2, y_2: coordinates at the end (downstream) of the subreach

By comparing the x and y values of the two points in question, we can determine the aspect of the stream. There are six possible cases, listed in the following table:

Flow Direction	Stream Aspect
Case 1: (x2 > x1)and (y2 > y1)	α
Case 2: ($x_2 > x_1$)and ($y_2 < y_1$)	$\Pi/2 - \alpha$
Case 3: ($x_2 < x_1$)and ($y_2 > y_1$)	$\Pi/2 + \alpha$
Case 4: ($x_2 < x_1$)and ($y_2 < y_1$)	$2\Pi - \alpha$
Case 5: ($x_2 > x_1$)and ($y_2 = y_1$)	$\Pi/2$
Case 6: ($x_2 < x_1$)and ($y_2 = y_1$)	$3\Pi/2$

Table 1.1 – Stream Aspect Cases

Once the stream aspect is known, the angles perpendicular to this orientation (azimuth angles) can be determined by simple adding or subtracting $\pi/2$. Figure

1.2 depicts the first two cases from Table 1 (L and R represent the right and left azimuth angles).

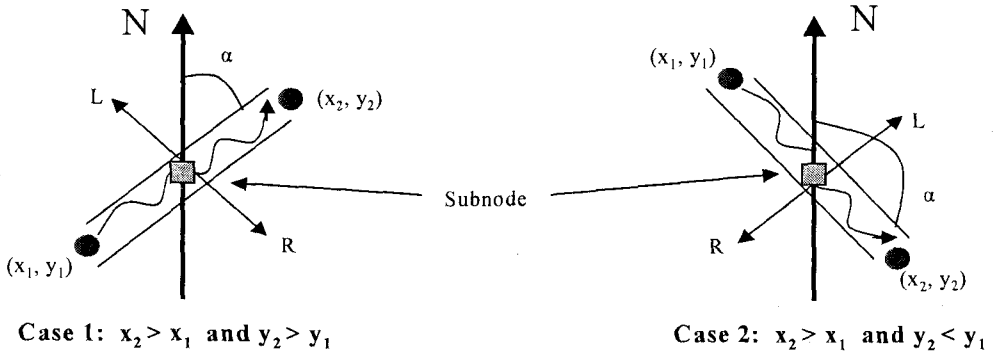

Figure 1.2 – Visual Representations of Cases 1 & 2 from Table 1.1

Topographic Shading

Topography surrounding streams provides shading, from only the earliest and latest parts of the day in areas with low topographic relief to most of the day in steeper canyons. Maximum angles of topographic shading in 8 main directions (offset by 45 degrees) are calculated at each subnode by WET-Temp during preprocessing. Due to the computational intensity of calculating topographic shading angles, they are directly interpolated from preprocessed values during a model run.

Calculation of these angles (Eq 1.2) is accomplished by stepping from the stream to the center of each adjacent DEM grid cell in a particular direction, recording the elevation, and calculating the shade angle between that cell and the stream.

$$\theta_{topoShade} = \arctan\left[\left(\frac{z_{new} - z_{subnode}}{d}\right)\right] \qquad \text{(Eq 1.2)}$$

where,

$\theta_{topoShade}$:	new topographic shading angle calculated
z_{new}:	elevation of the new DEM cell
$z_{subnode}$:	elevation of the stream at this subnode
d:	total distance stepped so far in this direction

The distance of each step is 10m when stepping N, E, S or W and 14.14 m when stepping NE, NW, SE or SW. The maximum topographic shading angle calculated in each of the 8 directions is associated with the subnode (Figure 1.3). Each small black dot radiating from the subnode represents one step through the DEM. These steps continue for 2km in each direction. This cutoff is meant to increase computational efficiency, with the assumption that topographic shading affects from beyond this distance are negligible.

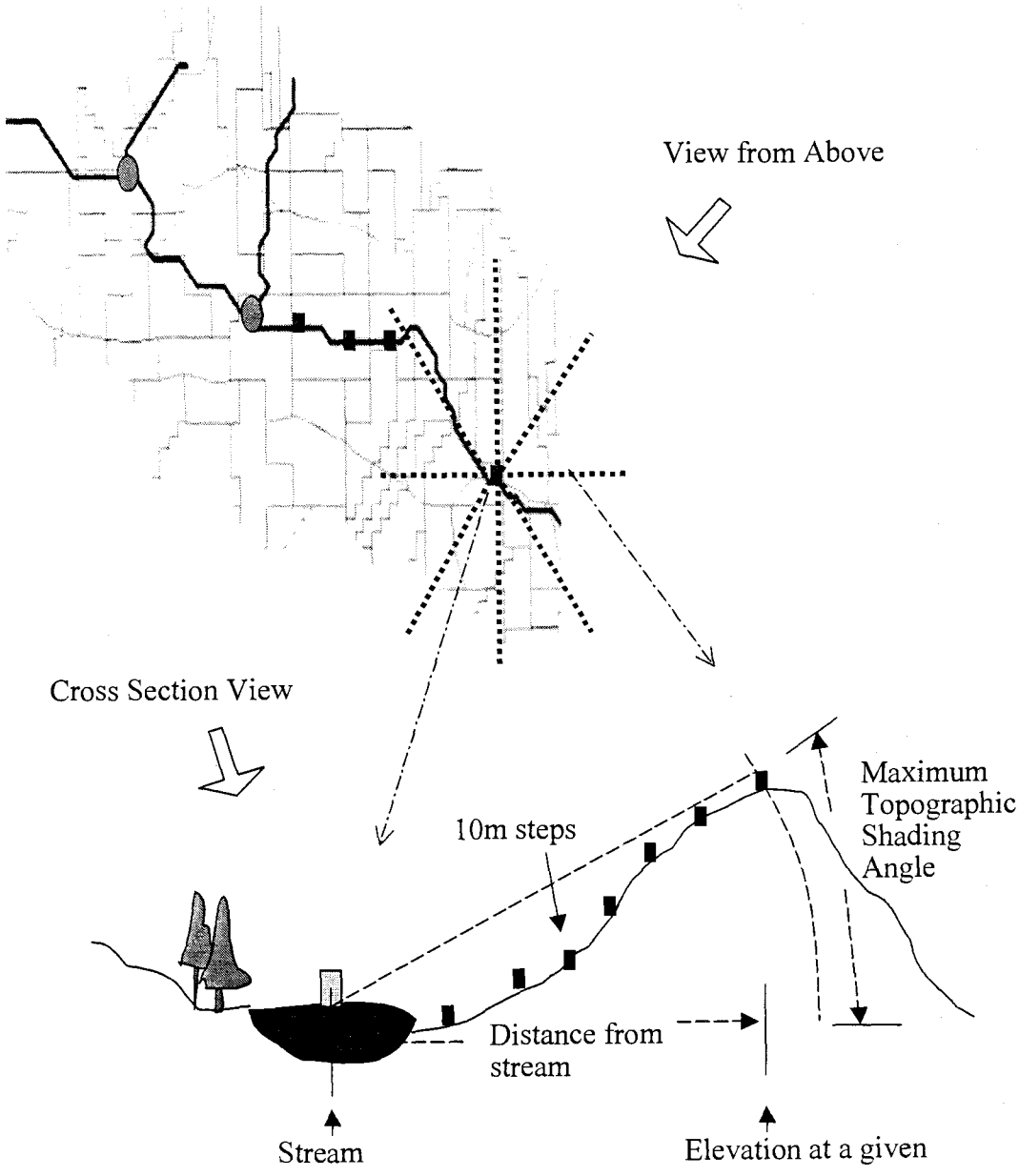

Figure 1.3 – Attributes used in topographic shading calculations in WET-Temp

Flow Estimation and Channel Geometry

Boyd (1996) found his reach-scale stream temperature model to be highly sensitive to changes in stream flow. It is generally acknowledged that low flow streams are more sensitive to temperature fluctuation than are high flow streams. Modeling stream temperature effectively requires a reasonable representation of flow and channel geometry.

Flow estimation in WET-Temp involves the distribution of observed discharge values throughout the stream network. The ratio of discharge to upstream basin area drained (specific discharge) is assumed to be constant throughout the network as each observed value is distributed upstream. Flow is distributed to the ends of the network (headwaters) or until another flow observation is reached. In the latter case, the new observed value is assigned to the current reach and distributed upstream. At this point, a new specific discharge value is calculated and used in subsequent upstream subreaches. A constraint of this method is that there must be a discharge measurement at the furthest downstream reach in the network.

Flow differentials between adjacent reaches are represented as lateral inflows distributed evenly to each subnode in the downstream reach. Lateral inflow values can be positive or negative depending on the flow differential. Negative lateral inflow values physically represent irrigation withdrawals and seepage into porous substrates. WET-Temp can take known point withdrawals and synthesize these with the flow estimation procedure. The withdrawn flow amount is added to total flow in the reach where the withdrawal occurs. This larger flow value is then distributed upstream.

Once stream discharge values across the basin have been estimated, calculation of wetted cross-sectional channel geometry (width and average depth) is possible. Calculation of average stream depth is based on the Gaukler-Manning equation (Eq 1.3). Rectangular geometry is assumed in WET-Temp, although other geometries (trapezoidal, triangular) can be used with this equation (Chanson, 1999).

$$\frac{Q}{w \cdot d} = \frac{1}{n} \cdot \left(\frac{A}{P_w} \right)^{2/3} (\sin \theta_{slope})^{1/2} \qquad \text{(Eq 1.3)}$$

where,

Q: stream flow (m^3/s)

n: manning's roughness coefficient (input by model user)

w: stream width

d: average stream depth

P_w: wetted perimeter (m, 2d + w for rectangular geometry)

A: cross sectional area(m^2, w*d for rectangular geometry)

θ_{slope}: angle of slope (radians)

Given the user input width/depth ratio (wdRatio) and the assumption of rectangular geometry, this equation can be solved for stream depth.

$$d = \left[\frac{Q \cdot n}{\sqrt{\sin \theta_{slope}} \cdot \left(\frac{wdRatio}{2 + wdRatio} \right)^{2/3} \cdot wdRatio} \right]^{3/8} \qquad \text{(Eq 1.4)}$$

$$w = d \cdot wdRatio \qquad \text{(Eq 1.5)}$$

Near Stream Disturbance Zone

The near stream disturbance zone (*nsdz*) is the distance between the nearest riparian vegetation on either side of the stream channel (see Figure 1.4). *Nsdz* width, necessary for calculating stream/vegetation geometric relationships, can be correlated with bankfull width (*bfw*). *Bfw* is estimated in each reach from the relationship obtained by regressing *Bfw* data against total area drained. Yearly high

flows tend to scour banks of vegetation, thus *nsdz* width is correlated with *bfw*, typically slightly wider.

Nsdz values will vary depending on the geomorphic features of the reach. A reach with low sinuosity and high gradient will generally have more a narrow *nsdz* than a more sinuous low gradient reach. Rosgen Level I (RL1) stream classifications, based on slopes, valley types, and channel patterns, are a convenient way to encompass these basic characteristics (Rosgen 1996). RL1 stream types can be assigned across the entire network using estimates of gradient and sinuosity derived from the stream and elevation datasets, as well as knowledge of the general geomorphic structures likely to occur in a particular watershed. *Nsdz* width is assigned as a certain percentage of estimated *BFW,* depending on the RL1 classification.

Given an *nsdz* estimate, the next step is calculation of the distance from the center of the stream to the nearest vegetation (distToVeg – Eq 1.6). Similar to topographic shading, this value is calculated in eight main directions and values are interpolated based on solar azimuth. The maximum value allowed is 30m, the distance to the next subnode.

$$distToVeg = \left| \frac{0.5 * nsdz}{\cos\theta} \right| \qquad \text{(Eq 1.6)}$$

$$\theta = \left| dirAng - nAA \right| \qquad \text{(Eq 1.7)}$$

where,

dirAngle: direction angle (North = 0°, then offset by 45 degrees)

nAA: nearest azimuth angle (either right or left)

Vegetation Parameters

Streamside vegetation reduces the input of solar radiation to the stream through reflection and absorption. The amount of solar radiation blocked is a function of the height, width, and density of streamside vegetation. Vegetation parameters are calculated during preprocessing, in eight directions offset by 45 degrees.

Vegetation information between these eight directions is directly interpolated during a model run.

In each direction, vegetation parameters are calculated within 100m of the stream, at 10m intervals. Maximum canopy height in areas modeled is significantly less than 100m, and it is assumed that amount of radiation attenuated beyond this 100m buffer is negligible due to low shading angles. The vegetation parameters (Figure 1.4, following page) include vegetation height, density, shading angle and height adjustment. Height and density are estimated using age, composition, dbh or other information from the particular vegetation coverage used. Height adjustment, taken from the DEM, is a measure of the elevation differential between the stream and each of the 10m increments. Vegetation shading angle (Eq 1.8) is calculated using the vegetation height and height adjustment. Maximum vegetation shade angle and maximum vegetation density are also recorded once for each of the 8 directions.

$$\theta_{vegShade} = \arctan\left[\left(\frac{h_{veg} + h_{adjust}}{dist}\right)\right] \qquad \text{(Eq 1.8)}$$

where,

$\theta_{vegShade}$: shade angle between top of vegetation and stream

h_{veg}: height of the vegetation

h_{adjust}: height differential between land surface and stream

dist: distance from stream

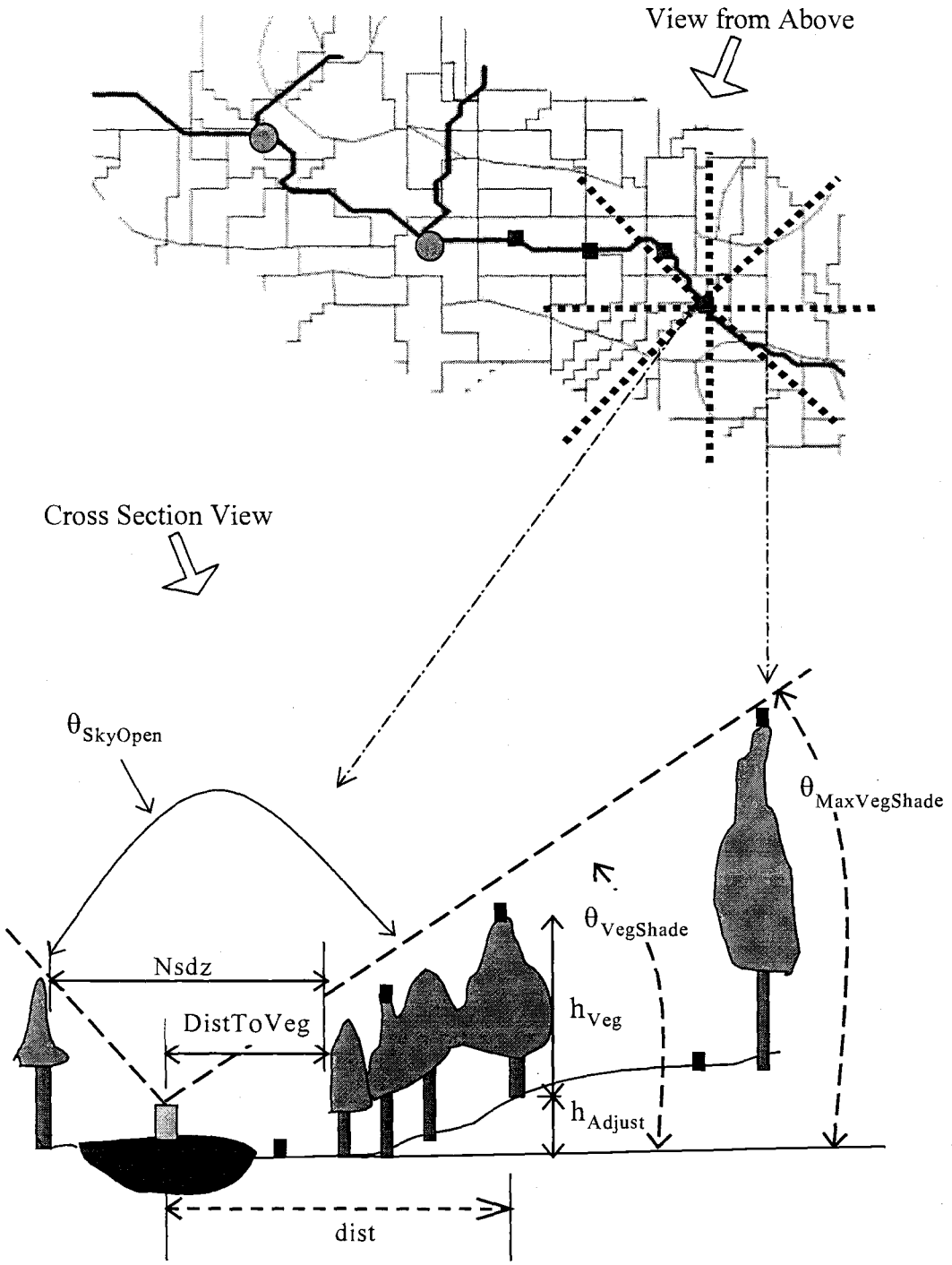

Figure 1.4 – Geometric relationships between the stream and riparian vegetation, used in the calculation of vegetation shading parameters for WET-Temp

Sky openness (Eq 1.9) is the amount of unblocked sky above a subnode, out of a possible 180 degrees. It is used in the calculation of diffuse radiation incident on the stream surface. Required for this calculation are vegetation and topographic shading, interpolated at both the right and left azimuth angles.

$$\theta_{skyOpen} = \pi - ((\max(\theta_{vegRight}, \theta_{topoRight}) + \max(\theta_{vegLeft}, \theta_{topoLeft})) \qquad \text{(Eq 1.9)}$$

where,

$\theta_{skyOpen}$:	sky Openness (radians)
$\theta_{vegRight/Left}$:	vegetation shade angle Right/Left
$\theta_{topoRight/Left}$:	topographic shade angle Right/Left
max:	maximum value of the two is used in the calculation

Energy Balance Calculations

Water temperature estimation at each subreach involves an energy balance for that subreach (Figure 1.5). The energy balance takes into account energy changes due to travel of water in and out of the subreach (advection) as well as thermodynamic heat flux processes within the subreach. Energy flow due to longitudinal mixing (physical dispersion) is assumed to be negligible. This assumption is valid for streams with low longitudinal temperature gradients and relatively high flow velocities, where advection dominates the advection/dispersion relationship (Sinokrot and Stefan 1993).

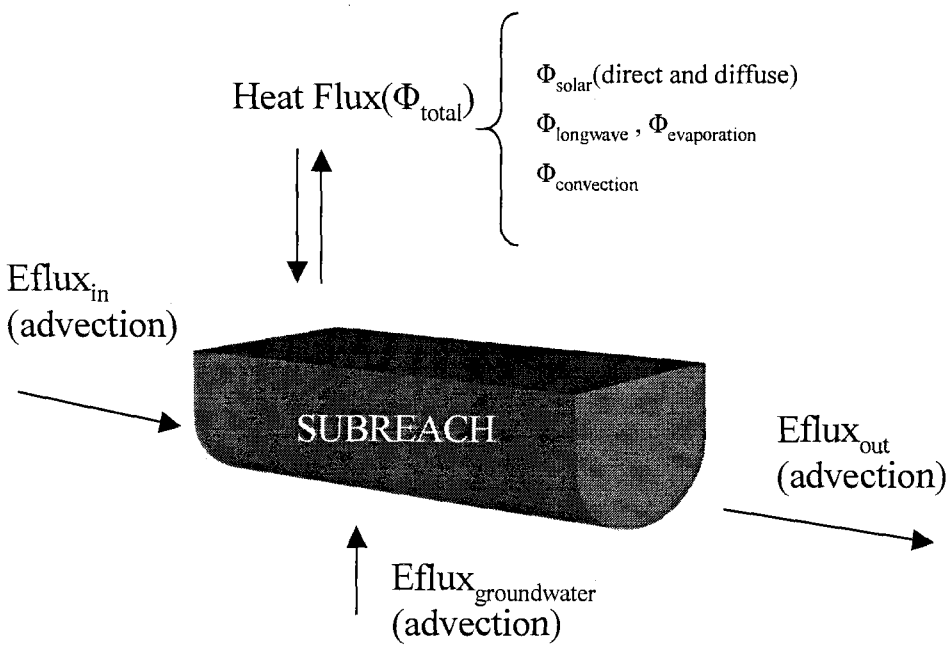

Figure 1.5 – Processes used to formulate the subreach energy balance in WET-Temp

Change in temperature per unit time for a control volume is expressed in Eq 1.11 (Boyd 1996).

$$\frac{\partial T}{dt} = \left(\frac{A \cdot \Phi_{total}}{\rho \cdot c_p \cdot V} \right) \qquad \text{(Eq 1.10)}$$

which simplifies to:

$$\frac{\partial T}{dt} = \left(\frac{\Phi_{total}}{\rho \cdot c_p \cdot D} \right) \qquad \text{(Eq 1.11)}$$

where,

A: stream cross-sectional area (m^2)

Φ_{total}: total heat flux ($kJ/m^2 \cdot s$)

ρ: water density (kg/m^3)

c_p: water heat capacity (kJ/kg·K)

V: volume(m^3)

D: depth(m)

A general energy balance on a stream segment considers these basic processes:

$$ChangeInEnergy = Advection + (Dispersion) + HeatFlux \qquad \text{(Eq 1.12)}$$

The energy balance, applied across the entire network, can be expressed in differential form (Eq 1.13).

$$\frac{\partial E}{dt} = \frac{\partial E}{dx} + \frac{\Phi_{total}}{\rho \cdot c_p \cdot D} \qquad \text{(Eq 1.13)}$$

The advection terms in Figure 1.4 can be expressed in terms of energy flux, with units of kJ/h (Eqs 1.14 - 1.16).

$$Eflux_{in} = Q_{in} \cdot T_{in} \cdot \rho \cdot c_p \cdot 3600 \qquad \text{(Eq 1.14)}$$

$$Eflux_{out} = Q_{out} \cdot T_t \cdot \rho \cdot c_p \cdot 3600 \qquad \text{(Eq 1.15)}$$

$$Eflux_{groundwater} = Q_{groudnwater} \cdot T_{groundwater} \cdot \rho \cdot c_p \cdot 3600 \qquad \text{(Eq 1.16)}$$

where,

Q = flow (m^3/s)

The four equations above are combined to arrive at the differential equation to be applied at each subnode in WET-Temp (Eq 1.17).

$$\frac{\partial E}{dt} = Eflux_{in} + Eflux_{groundwater} - Eflux_{out} + \frac{\Phi_{total}}{\rho \cdot c_p \cdot D} \qquad \text{(Eq 1.17)}$$

Heat Flux Calculation

The total heat flux term in the energy balance (Φ_{total}) represents the rate of energy gained or lost by a subreach per unit area via processes other than advection. Expressed in ($kJ/m^2 \cdot h$), it is estimated by summing the contributions of individual heat flux processes. WET-temp takes into account the effects of terrestrial and atmospheric long-wave radiation, evaporation, convection, and short-wave solar radiation.

Longwave Radiation Flux

All terrestrial bodies emit and absorb radiation based their temperature and apparent emissivity. The emissivity of a terrestrial body is defined as the fraction of the maximum possible longwave radiation emission at a particular temperature (Oke 1978). In essence, each body radiates as a blackbody (emmisivity = 1.0) at some temperature lower than its actual temperature. The longwave radiation (3 to 100μm) emitted by the atmosphere ($\Phi_{atmLongwaveTotal}$), the stream ($\Phi_{streamLongwave}$), and the streamside vegetation ($\Phi_{vegLongwave}$) are quantified in WET-temp. Longwave radiation emitted by the stream (back radiation) is calculated using the Stefan-Boltzmann radiation law.

$$\Phi_{streamLongwave} = \varepsilon_{stream}\sigma(T_s + 273)^4 \qquad \text{(Eq 1.18)}$$

where,

$\Phi_{streamLongwave}$: Back radiation from stream

ε_{stream}: emissivity of water (assumed to be 0.97)

σ: Stefan-Boltzmann constant (5.67×10^{-8} $W \cdot m^{-2} \cdot K^{-4}$)

T_s: Stream Temperature (°C)

Longwave radiation emitted from streamside vegetation (Eq 1.19a,b) is calculated assuming the temperature of the vegetation the same as that of the surrounding surrounding atmosphere.

$$\Phi_{vegLongwaveRight} = \varepsilon_{veg} \cdot \sigma \cdot (\rho Veg_{right} \cdot \theta_{VegShadeRight}) \cdot (T_{veg} + 273)^4 \quad \text{(Eq 1.19a)}$$

$$\Phi_{vegLongwaveLeft} = \varepsilon_{veg} \cdot \sigma \cdot (\rho Veg_{Left} \cdot \theta_{VegShadeLeft}) \cdot (T_{veg} + 273)^4 \quad \text{(Eq 1.19b)}$$

where,

$\Phi_{vegLongwave}$: long-wave radiation emitted from vegetation

$\rho Veg_{left/right}$: vegetation density left/right

$\theta_{VegShadeLeft/Right}$: vegetation shade angle left/right

T_{veg}: vegetation temperature (same as T_{air})

ε_{veg}: vegetation emissivity (assumed to be 0.95)

Atmospheric longwave radiation is mainly dependent on the amount of water vapor in the atmosphere and the air temperature. Particulates and other atmospheric chemicals also have small influences (McCutcheon 1989). Empirical studies have shown that under clear skies the atmosphere tends to emit as a blackbody with a temperature 20° C lower than the surface air temperature, while under cloudy skies this apparent radiating temperature is only 2° C lower than surface air temperature (Jones 1983). This apparent radiating temperature, used to calculate atmospheric longwave radiation, is represented by WET-Temp as varying with relative humidity between 2 and 20 degrees (Eq 1.20a-c). Atmospheric longwave coming from the sky opening (Eq 1.20a) as well as from gaps in the left bank and right back vegetation (Eqs 1.20b,c) is calculated.

$$\Phi_{atmLongOpen} = \sigma \cdot ((T_{air} - \left(20 \cdot \left(0.9 \cdot \frac{RH}{5}\right)\right) + 273)^4 \cdot \left(\frac{\theta_{skyOpen}}{\Pi}\right) \quad \text{(Eq 1.20a)}$$

$$\Phi_{atmLongL} = \sigma \cdot ((T_{air} - \left(20 \cdot \left(0.9 \cdot \frac{RH}{5}\right)\right) + 273)^4 \cdot \left(\frac{\theta_{vegShadeL}}{\Pi}\right) \cdot \rho Veg_L \quad \text{(Eq 1.20b)}$$

$$\Phi_{atmLongR} = \sigma \cdot ((T_{air} - \left(20 \cdot \left(0.9 \cdot \frac{RH}{5}\right)\right) + 273)^4 \cdot \left(\frac{\theta_{vegShadeR}}{\Pi}\right) \cdot \rho Veg_R \quad \text{(Eq 1.20c)}$$

$$\Phi_{atmLongwaveTotal} = \Phi_{atmLongOpen} + \Phi_{atmLongR} + \Phi_{atmLongL} \quad \text{(Eq 1.20d)}$$

where,

$\Phi_{atmLongwaveTotal}$: total atmospheric longwave radiation

$\Phi_{atmLongR}$: atmospheric longwave radiation, vegetation gaps on right

$\Phi_{atmLongL}$: atmospheric longwave radiation, vegetation gaps on left

$\Phi_{atmLongOpen}$: atmospheric longwave radiation from sky opening

T_{air}: Air temperature

C_f: Cloud fraction (input by model user)

Evaporative Flux

A vapor gradient between a water body and the drier air above it drives evaporation. Le Chatelier's principle predicts that water molecules will travel from the water surface (area of greater water concentration) to the air above (area of lower water concentration), in an attempt to reach equilibrium. Each time a molecule of water changes from liquid to vapor, it gains (and therefore the stream loses) energy amounting to its latent heat of vaporization. If the air above becomes supersaturated due to a decrease in air or water temperature, heat can be transferred back to the water body via condensation.

Evaporative heat flux (Eq 1.21) is thought to be most important factor in the dissipation of elevated surface water temperatures (McCutcheon 1989).

$$\Phi_{evaporation} = \gamma LE \quad \text{(Eq 1.21)}$$

where,

$\Phi_{evaporation}$: Evaporative heat flux

γ: Specific gravity of water (constant : 1000 kg/m^3)

L: latent heat of vaporization

E: evaporation rate

Latent heat of vaporization is dependent on the temperature of the water column (T_{stream}), and is approximated (Eq 1.22) by regressing T_{stream} against values of latent heat obtained from steam tables (Geankoplis 1993).

$$L = 2501.4 + (1.83 * T_{stream}) \qquad \text{(Eq 1.22)}$$

Air temperature, wind speed and relative humidity are the climatic parameters used in the estimation of evaporation rate (Eq 1.23). These climatic parameters must be estimated using the closest available climatic data for the basins where WET-Temp is to be applied. Scores of relationships have been developed to fit the two empirical parameters in Eq 23. Most of these have been developed over lakes and reservoirs. Bowie et al (1985) presented a formula (Eq 1.24) used in modeling evaporation on the San Diego aqueduct. In further studies involving moving waters the empirical parameters preceding wind speed (EvapA, EvapB) had to be altered to reflect different climatic conditions, so WET-Temp allows the user to adjust these coefficients depending on the area of study.

$$E = (EvapA + EvapB \cdot u)(e_s - e_a) \qquad \text{(Eq 1.23)}$$

where,

E: evaporation rate (mm/day)

EvapA, EvapB: empirical coefficients input by model user

u: wind speed

e_s: saturation vapor pressure

e_a: atmospheric vapor pressure

$$E = 3.01 + 1.13u(e_s - e_a) \qquad \text{(Eq 1.24)}$$

Transfer of molecules across the air water interface is spurred by the intensity of water molecule motion. This factor determining this motion is temperature, thus, assuming constant atmospheric pressure, saturation vapor pressure (Eq 1.25) can be expressed as a function of surface (air) temperature (T_{air}).

$$e_s = \exp\left[2.3026\left(\frac{aT_{air}}{T_{air} + b} + c\right)\right] \qquad \text{(Eq 1.25)}$$

Relative humidity is defined as the ratio of atmospheric vapor pressure to saturation vapor pressure (Dingman 1994). Given relative humidity data and saturation vapor pressure, this relationship can be used to determine atmospheric vapor pressure (Eq 1.26).

$$e_a = \left(\frac{RH * e_s}{100}\right) \qquad \text{(Eq 1.26)}$$

where,

RH: relative humidity (%)

Convective Flux

Convective heat transfer involves the bulk transport and mixing of warmer and cooler portions of a fluid (Geankoplis 1993). Convection at the air-water interface occurs at a rate proportional to a temperature gradient (present when the air and water are at different temperatures) as described by Fourier's classic heat transfer studies. The process is not measurable in the field and must be inferred from measurements of other processes. The Bowen ratio (Eq 1.27), a constant of proportionality between evaporative and convective heat flux, is the most convenient method for this purpose (Boyd 1996; McCutcheon 1989).

$$BowenRatio = \frac{\Phi_{convection}}{\Phi_{evaporation}} = 0.01 \cdot \left[\frac{T_{stream} - T_{air}}{e_s - e_a}\right] \cdot \left[\frac{P_{atm}}{29.92}\right] \quad \text{(Eq 1.27)}$$

where,

P_{atm}: total atmospheric pressure (corrected for elevation)

Solar Flux

The largest component of radiation incident on the surface of the earth is short wave solar radiation (with both direct and diffuse components). It follows that this solar radiation is the single largest source of energy available to elevate stream temperatures (Beschta 1997, Sinokrot and Stefan 1993). The quantity of energy that is transferred to the stream water column is diminished by riparian vegetation interception, topographic interception, and stream reflectance (albedo).

The first step toward quantifying solar energy imparted to a stream is the determination of the solar position relative to the stream. At the base of most solar calculations is the Julian day or calendar day, ranging from 1 to 365. Solar declination (Eq 1.28) is a measure of the angle between 2 lines: the line between the center of the earth and the center of the sun, and a line along the equatorial plane of the earth (see Appendix A2).

$$\delta = 23.45 \sin((\frac{\Pi}{180}) * (\frac{360}{365}) * (284 + julianDay)) \qquad \text{(Eq. 1.28)}$$

where,

δ: declination

One solar day is the time it takes for the sun to complete one cycle around a stationary point on earth. This is not necessarily 24 hours, and can vary throughout the year by up to 16 minutes (Iqbal 1983). The equation of time (Eq 1.29a,b) is an empirical factor used to convert local standard time into solar time (Eq 1.31). A

longitude correction (Eq. 1.30) is also needed because standard time is uniform across a time zone while solar time is not (Hsieh 1986). This correction consists of four minutes for each degree of distance from the standard longitude. WET-Temp's time step units are fractions of days. Local standard time is calculated by taking the fractional component of the time step and converting units from days to hours.

$$E_t = (9.87 \sin 2B - 7.53 \cos B - 1.5 \sin B)/60 \qquad \text{(Eq 1.29a)}$$

$$B = \frac{360}{364}(JulianDay - 81) \qquad \text{(Eq 1.29b)}$$

where,

E_t: Equation of time (hours)

$$Lc = 4(L_s - L_l)/60 \qquad \text{(Eq 1.30)}$$

where,

Lc: longitude correction (hours)

L_s: standard longitude (degrees)

L_l: local longitude (degrees)

$$t_{solar} = LST + E_t + Lc \qquad \text{(Eq 1.31)}$$

where,

LST: local standard time

t_{solar}: solar time (hours)

A meridian is a circle drawn (figuratively) through the poles of a celestial sphere. On earth, these are our lines of longitude. Hour angle (Eq 1.32) is a measure of the angle the earth would have to turn through to bring the sun directly above the observer's meridian. This has a value of zero at solar noon and varies

15° per hour, with positive values occurring before and negative values after solar noon (Hsieh 1986; Iqbal 1983).

$$H = (12 - t_{solar}) * 15 * (\frac{\Pi}{180}) \qquad \text{(Eq 1.32)}$$

where,

H: hour angle (radians)

Hour angle, declination and latitude (see Appendix 1B) make up the three basic solar geometric angles. Three derived geometric angles (see Appendix 1B) are also important in solar calculations. These are azimuth, solar altitude and zenith angle (Hsieh 1986). Solar altitude (Eq 1.33) is the angle between the line joining the observer and the sun and the observer's celestial horizon. Zenith angle is the complement of solar altitude. Solar altitude has a zero value before sunrise and after sunset.

$$\alpha = \sin^{-1}[\sin\delta * \sin L + \cos\delta * \cos L * \cos H] \qquad \text{(Eq 1.33)}$$

where,

L: latitude (radians)

α: Solar altitude (radians)

Solar azimuth (Eq 1.34) can be thought of as the angle between the sun's rays and the observer's meridian, measured in the horizontal plane (Hsieh 1986).

$$\phi = \sin^{-1}\left[\cos\delta\left[\frac{\sin H}{\cos\alpha}\right]\right] \qquad \text{(Eq 1.34)}$$

where,

ϕ: solar azimuth (radians)

Once solar position is determined, the next step is the calculation of radiation at the earth's surface. This is done in two steps, first calculating the radiation at the edge of the atmosphere and then estimating the amount that penetrates the

atmosphere. Radiation at the atmosphere's edge is termed extra-terrestrial radiation (Eq 1.36). An eccentricity factor (Eq 1.35) is necessary to account for the fact that the orbit of the earth around the sun is not quite circular, but elliptical, which slightly alters the solar constant throughout the year (Iqbal 1983).

$$E_o = 1 + 0.033 \cos\left[\frac{2\Pi * julianDay}{365}\right] \quad \text{(Eq 1.35)}$$

$$I_{et} = H_{sc} * E_o * \sin\alpha \quad \text{(Eq 1.36)}$$

where,

H_{sc}: solar constant = 4781 (kJ/m^2*h)

I_{et}: extra-terrestrial (kJ/m^2*h)

Aerosols and other atmospheric particles attenuate extra-terrestrial radiation before it reaches the surface of the earth. The transmissivity (Eq 1.39) of the atmosphere estimates the fraction of I_{et} that remains unattenuated. Relative optical air mass (Eq 1.37), a term used in the evaluation of atmospheric attenuation is equivalent to the path length through the atmosphere (Iqbal 1983). This term must be corrected for elevation (Eq 1.38).

$$m_r = \frac{35}{(1224\sin\alpha + 1)^{0.5}} \quad \text{(Eq 1.37)}$$

where,

m_r: relative optical air mass (dimensionless)

$$m = m_r * \exp(-0.0001184 * z) \quad \text{(Eq 1.38)}$$

where,

z: elevation (meters)

m: optical air mass corrected for elevation (dimensionless)

$$A_t = 0.0685 \cos\left[\frac{2\Pi}{365}(julianDay + 10)\right] + 0.80 \quad \text{(Eq 1.39)}$$

where,

A_t: atmospheric transmissivity

The estimation of the atmospheric transmissivity now allows us to formulate an expression (Eq 1.40) for radiation at the surface of the earth (Wunderlich 1972, Boyd 1996).

$$I_{surface} = I_{et} * A_t^m \quad \text{(Eq 1.40)}$$

where,

$I_{surface}$: radiation at earth's surface (kJ/m^2*h)

As solar radiation enters the earth atmosphere, some is scattered and some is absorbed. The scattered radiation, known as diffuse radiation, is either reflected back to space or toward the ground. The radiation associated with the apparent disk of the sun is known as direct radiation. Total radiation present at the earth's surface must be partitioned into direct (Eq 1.43) and diffuse (Eq 1.41a/b, Eq 1.42) radiation (Chen 1994).

$$DF = 0.938 + 1.071K_T - 5.146K_T^2 + 2.982K_T^3 - (0.009 - 0.078K_T)\sin[X] \quad \text{(Eq 1.41a)}$$

$$X = \frac{2\Pi(julianDay - 40)}{365} \quad \text{(Eq 1.41b)}$$

where,

DF: diffuse fraction (dimensionless)

K_T: $I_{surface}/I_{et}$ (dimensionless)

$$I_{diffuse} = DF * I_{surface} \quad \text{(Eq 1.42)}$$

$$I_{direct} = I_{surface} - I_{diffuse} \quad \text{(Eq 1.43)}$$

The fraction of solar radiation attenuated during its path through the riparian canopy must be estimated. Radiation attenuation by vegetation is a function of the height and density of the vegetation. Path length of the solar beam through the streamside vegetation must be estimated to calculate radiation attenuated. The calculation of path length is performed at the bounding 45-degree direction intervals, and the results are interpolated.

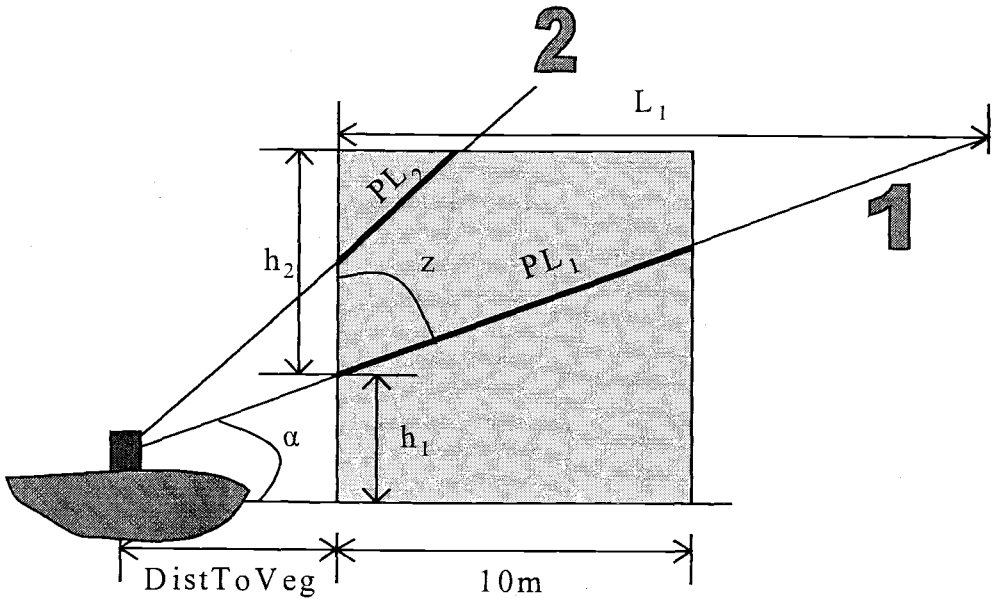

Figure 1.6 – WET-Temp path length calculation

Vegetation in WET-Temp is essentially represented as 10m blocks with certain heights and densities. Depending on the solar altitude, the solar beam can pass through the 10m block starting from the side (Figure 1.6, PL_1) or from the top (Figure 1.6, PL_2). The next several equations are used to estimate path length. α

and z represent solar altitude and zenith angle respectively, while h_{veg} represents total vegetation height.

$$h_1 = distToVeg \cdot \tan(\alpha) \quad \text{(Eq 1.44)}$$

$$h_2 = h_{veg} - h_1 \quad \text{(Eq 1.45)}$$

$$z = 90 - \alpha \quad \text{(Eq 1.46)}$$

$$L_1 = h_2 \cdot \tan(z) \quad \text{(Eq 1.47)}$$

In case 1 above, L_1 is greater than 10. In this case the path length (PL_1) can be calculated with Eq 1.48.

$$PL_1 = 10 / \cos(\alpha) \quad \text{(Eq 1.48)}$$

In case 2 above, L_1 is less than 10, and PL_2 is calculated with Eq 1.49 (noting that the values of α and z will be different than case 1).

$$PL_2 = h_2 / \cos(z) \quad \text{(Eq 1.49)}$$

The above procedure is repeated for every contributing 10m vegetation block (i.e. $\theta_{vegShade} > \alpha$) at each time step. Effective vegetation density is simply the average of all the contributing vegetation blocks.

Beschta and Weatherred (1984) empirically fit equations for stream albedo (Eq 1.50a,b) as a function of solar altitude based on data from Sellars (1965).

$$a_{stream} = 0.091\left(\frac{1}{(\cos(1-\alpha)}\right) - 0.0386 \qquad (0° < \alpha < 80°) \qquad \text{(Eq 1.50a)}$$

$$a_{stream} = (0.0515 \cdot \alpha) - 3.635 \qquad (80° < \alpha < 90°) \qquad \text{(Eq 1.50b)}$$

where,

a_{stream}: stream albedo (dimensionless)

While passing through a homogeneous medium, radiation is attenuated according to Beer's Law (Iqbal 1983). Chen (1996) estimated an extinction

coefficient (Eq 1.52) and used Beer's Law (Eq. 1.51) to calculate radiation attenuation in a riparian canopy.

$$\Phi_{belowCanopy} = \Phi_{aboveCanopy} e^{-k * pathLength} \quad \text{(Eq 1.51)}$$

$$k = \frac{-\ln(1 - \rho_{effective}/100)}{havg_{apparent}} \quad \text{(Eq 1.52)}$$

where,

$\Phi_{belowCanopy}$: radiation flux below vegetation canopy

$\rho_{effective}$: effective vegetation density

$havg_{apparent}$: average height of vegetation + h_{adjust}

k: extinction coefficient

$$I_{attenuated} = \frac{\Phi_{belowCanopy}}{\Phi_{aboveCanopy}} = e^{-k * pathLength} \quad \text{(Eq 1.53)}$$

Total solar radiation (Eq 1.56) is a combination of diffuse solar radiation and beam solar radiation. Diffuse radiation can enter the water column from the sky opening (Eq 1.54) as well as through gaps in the vegetation (Eq 1.55).

$$\Phi_{diffuseOpen} = \theta_{skyOpen} * I_{diffuse} \quad \text{(Eq 1.54)}$$

$$\Phi_{diffuse(Right/Left)} = (1 - \rho Veg_{Right/Left}) * \theta_{shaded(Right/Left)} * I_{diffuse} \quad \text{(Eq 1.55)}$$

where,

$$\theta_{shaded} = \theta_{vegShade} - \theta_{topoShade}$$

$$\Phi_{solar} = (\Phi_{beam} \cdot I_{attenuated} + \Phi_{diffuseOpen} + \Phi_{diffuseRight+Left}) \cdot a_{stream} \quad \text{(Eq 1.56)}$$

Model Use and Outputs

The model user sets the simulation time step, starting time and stopping time. The following list contains input parameters the model user is required to provide. These parameters can be adjusted within reasonable bounds to calibrate the model to a particular basin.

- Evaporation Coefficient A (EvapA)
- Evaporation Coefficient B (EvapB)
- Groundwater Temperature
- Manning's roughness coefficient (Manning's n)
- Cloud fraction
- Width/Depth ratio
- Volume Multiplier (see text below)
- Flow Multiplier (see text below)

Subreach volumes are derived from stream discharge values, and can be under-predicted because water residing in the subreach is not accounted for. A volume multiplier is included as a model input to allow adjustment for this situation. The flow multiplier is a tool that can be used to examine the impacts of flow change on temperature distributions.

Model output exists is two forms, time series and longitudinal profiles. Time series outputs, collected only at reaches specified by the model user, include temperature and components of the energy balance. Longitudinal profile data includes stream temperature, flow, subreach residence time, and lateral inflow. Longitudinal profiles are available for the time of day the model is stopped. Flow, lateral inflow and residence time are unchanging with time as modeled in this paper, but can provide interesting insights when compared to stream temperature profiles. Residence times across the network are important because the minimum subreach residence time in the system effectively sets the maximum time step

available to the model user. Stream temperature profiles from several identical runs stopped at different times of day can be used to examine changes in temperature distribution over time.

Summary

The development of WET-Temp provides a stream temperature model that fully utilizes spatially distributed data. The model represents the stream as a network rather than an aggregation of individual reaches, allowing for dynamic watershed scale analyses than have been impossible previously. WET-Temp calculates stream temperature responses to land use changes at fine spatial resolution (30m) across the network.

WET-Temp relies on the robust description of solar position with respect to streamside vegetation in order to quantify solar radiation input to the water column. The relative contributions of other heat flux processes (evaporation, convection, conduction and longwave radiation) are considered in order to more accurately estimate the total heat flux at a stream subreach.

Managers and watershed groups can use WET-Temp to perform watershed scale simulations and identify temperature trouble spots. They will be able to evaluate the size and location of restoration alternatives needed to accomplish particular stream temperature goals. Through the incorporation of spatially explicit datasets, WET-Temp advances the state of the art in watershed scale stream temperature modeling.

References

Bartholow, J.M. 1990. Stream temperature model. Pages IV-20 to IV-47 in W.S. Platts ed. Managing Fisheries and Wildlife on Rangelands grazed by Livestock: A guidance and reference document for biologists. W.S. Platts and Assoc. for the Nevada Department of Wildlife. December, 1990. v.p.

Bartholow, J.M. 1995. The stream network temperature model (SNTEMP): A decade of results. Pages 57-60 *in* Ahuja, L., K. Rojas and E. Seely, editors. Workshop on Computer Applications in the Water Management, Proceedings of the 1995 Workshop. Water Resources Research Institute, Fort Collins, Colorado. Information Series No. 79. 292 pp.

Belksy, A.J., A. Matzke and S.Uselman. 1999. Survey of livestock influences on stream and riparian ecosystems in the western United States. Journal of Soil and Water Conservation 54(1) : 419-431.

Beschta, R.L. and J. Weatherred. 1984. A computer model for predicting stream temperatures resulting from the management of streamside vegetation. *USDA Forest Service.* WSDG-AD-00009.

Beschta, R.L., R.E. Bilby, G.W. Brown, L.B. Holtby and T.D. Hofstra, 1987. Stream Temperature and Aquatic Habitat : Fisheries and Forestry Interactions. *In* Streamside Management : Forestry and Fisheries Interactions, E.O. Salo and T.W. Cundy (Editors). Contribution No. 57, University of Washington, Institute of Forest Resources, 471 pp.

Beschta, R.L. 1997. Riparian Shade and Stream Temperature: An Alternative Perspective. *Rangelands* 19(2): 25-28.

Bowie, G.L., Mills, W.B., Porcella, D.B., Campbell, C.L., Pagenkopf, J.R., Rupp, G.L., Johnson, K.M., Chan, P.W., and S.A. Gherini. 1985. Rates, Constants, and Kinetics Formulations in Surface Quality Modelling, 2nd Edition. EPA/600/3-85/040, U.S. Environmental Protection Agency, Athens, GA.

Boyd, M. 1996. Heat Source : Stream, River and Open Channel Temperature Prediction. Master's thesis at Oregon State University, Department of Bioresource Engineering/Civil Engineering.

Brown, George W. 1969. Predicting Temperatures of Small Streams. Water Resources Research. 5(1) : 68-75.

Brown G.W. and J.T. Krygier. 1970. Effects of Clear-Cutting on Stream Temperatures. Water Resources Research 6(4) : 1133-1140.

Brunke, M., and T. Gonser. The ecological significance of exchange processes between rivers and groundwater. Freshwater Biology. 37 : 1-33.

Carnahan, B., Luther, H.A., Wilkes, J.O. 1969. Applied Numerical Methods. John Wiley and Sons, New York, 603pp.

Chanson, H. 1999. The Hydraulics of Open Channel Flow. Arnold, London, 495pp.

Chen, Y.D. 1996. Hydrologic and water quality modeling for aquatic ecosystem protection and restoration in forest watersheds: a case study of stream temperature in the Upper Grande Ronde River, Oregon. PhD dissertation, University of Georgia, Athens, Ga.

Chen, Y.D., R.F. Carsel, S.C. McCutcheon, and W.L. Nutter. 1998. Stream Temperature Simulation of Forested Riparian Areas: I. Watershed-Scale Model Development. Journal of Environmental Engineering 124(4) : 304-315.

Chen, Y.D., S.C. McCutcheon, D.J. Norton and W.L. Nutter. 1998. Stream Temperature Simulation of Forested Riparian Areas : II. Model Application. Journal of Environmental Engineering 124(4) : 316-328.

Dingman, S.L. 1994. Physical Hydrology. Prentice Hall, New Jersey, 556pp.

Hauer F.R. and G.A. Lamberti. 1996. Methods in Stream Ecology. Academic Press, San Diego, 674pp.

Horne, A.J. and C.R. Goldman. 1994. Limnology, 2nd edition. McGraw-Hill Inc., New York, 575pp.

Hsieh, J. 1986. Solar Energy Engineering. Prentice Hall Inc., New Jersey, 553pp.

Iqbal, M. 1983. An introduction to solar radiation. Academic Press, Toronto, 390pp.

Jones, H.G. 1983. Plants and Microclimate. A quantitative approach to environmental plant physiology. Cambridge University Press, Cambridge, 323pp.

LeBlanc, R.T., R.D. Brown, and J.E. FitzGibbon. 1997. Modeling the effects of land use change on the water temperature in unregulated urban streams. Journal of Environmental Management 49(4) : 445-469.

McCuthceon, S.C. 1989. Water Quality Modelling: Vol. 1, Transport and Surface Exchange in Rivers. CRC Press, Boca Raton, 334 pp.

McIntosh, B.A. 1992. Historical changes in anadromous fish habitat in the Upper Grande Ronde River, Oregon, 1941-1990. MS Thesis, Oregon State University, Corvallis, OR.

National Marine Fisheries Service. Feb 2, 2000. Northwest Region Species List (Endangered, Threatened, Proposed, and Candidate Species under National Marine Fisheries Service Jurisdiction that Occur in Oregon, Washington, and Idaho). Retrieved March 11, 2002 from http://www.nwr.noaa.gov/1habcon/habweb/listnwr.htm.

Natural Resources Conservation Service. June 13.2001. Soil Survey Geographic (SSURGO) Database. Retrieved March 22, 2002 from http://www.ftw.nrcs.usda.gov/ssurgo.html.

Northwest Power Planning Council (NPPC). 1992. Strategy for salmon, volumes I and II. Portland, OR.

Oetter, D.R., W.B. Cohen, M. Berterretche, T.K. Maiersperger and R.E. Kennedy. 2001. Land cover mapping in an agricultural setting using multi-seasonal Thematic mapper data. Remote Sensing of Environment 76(2):139-155.

Oregon Department of Environment Quality. 1998. Oregon DEQ 303(d) list of water quality limited streams and stream segments – Streams Summary Report. Retrieved March 11, 2002 from htttp://www.deq.state.or.us/wq/303dlist/StreamsSummaryReport.htm

Ritchey, D. 2000. Design and Prioritized Implementation of Woody Riparian Buffers for Increasing Effective Shade in Agricultural Landscapes of the Willamette River Valley, Oregon. Masters Project. University of Oregon, Eugene, OR.

Rosgen, D. 1996. Applied River Morphology. Wildland Hydrology, Pagosa Springs, CO.

Schroeter, H.O., D.J. Van Vliet, K. Boehmer and D. Beach. 1996. Continuous in-stream temperature modeling: Integration with a physically based subwatershed

hydrology model. Advances in Modeling the Management of Stormwater Impacts., Ann Arbor Press, Inc. Chelsea, MI, pp. 27-48.

Sellars, W.D. 1965. Physical Climatology. University of Chicago Press, Chicago. 272 pp.

Sinokrot, B.A. and H.G. Stefan. 1993. Stream Temperature Dynamics : Measurements and Modeling. Water Resources Research. 29(7) : 2299-2312.

Sullivan, K. and T.N. Adams. 1991. The Physics of Stream Heating: 2) An analysis of temperature patterns in stream environments based on physical principles and field data. Weyerhaeuser Technical Report 044 -5002/89/2.

Theurer, F.D., K.A. Voos, and W.J. Miller. 1984. Instream Water Temperature Model. Instream Flow Information Paper 16. U.S. Fish and Wildlife Service. FWS/OBS-84/15. 200 pp.

Wilson, W.J., M.D. Kelley, and P.R. Meyer. 1987. Instream temperature modeling and fish impact assessment for a proposed large-scale Alaska hydroelectric project. Pages 183-206 *in* J.F. Craig and J.B. Kemper, eds. Regulated streams. Plenum Press, New York, 431 pp.

Appendices

Appendix 1A – Parameter Spatial Extent

Cells created from intersection of:
SSURGO soil coverage
Watershed delineations (5 ha threshold area)
30m vegetation grid (USGS/PNWERC, from LANDSAT images. Ground validated.)

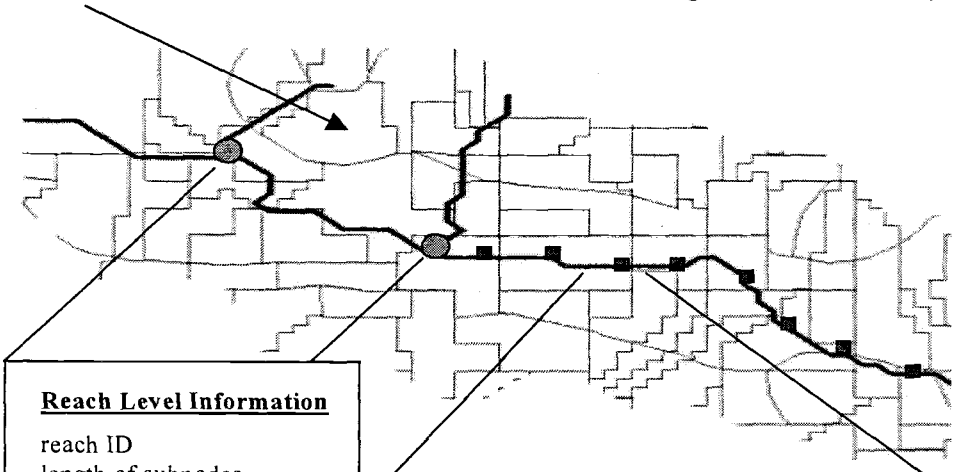

Reach Level Information

reach ID
length of subnodes
subnode count
stream order
reach length
slope
upstream node location (x,y)
gradient
sinuosity
Rosgen Level I stream type

Subreach Level Information

Time Invariant Information

-Topographic Shading (8 directions)
-Stream Aspect
-Stream Discharge
-Sky Openness
-Left/Right Azimuth Angles
-Left/Right Vegetation Shading Angles
-Left/Right Topographic Shading Angles
-Subnode Elevation
-Subnode Location (x,y)
-Vegetation Information (8 directions)
  Shading Angle (10 values in each direction)
  Density (10 values)
  Veg Height (10 values)
  Height Adjustment (10 values)
  Maximum Shade Angle
  Maximum Density
  Average Height
  Distance to Vegetation

Figure 1A.1 – Spatial Extent of Time Invariant Parameters

Appendix 1B – Basic and Derived Solar Angles

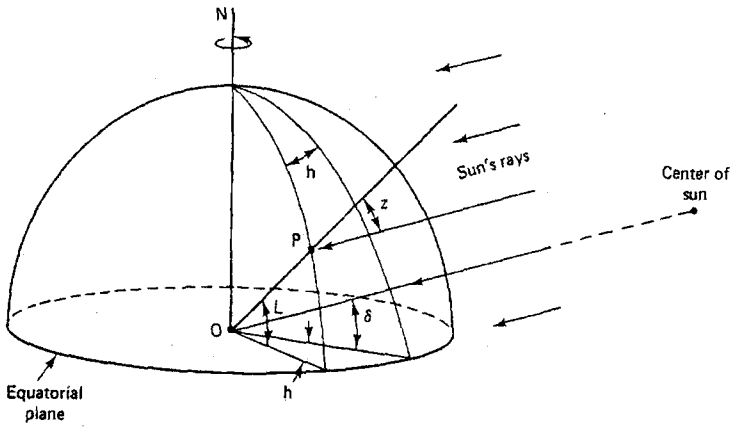

Figure 1B.1 – Basic Solar Angles

L: Latitude h: Hour Angle δ: Declination

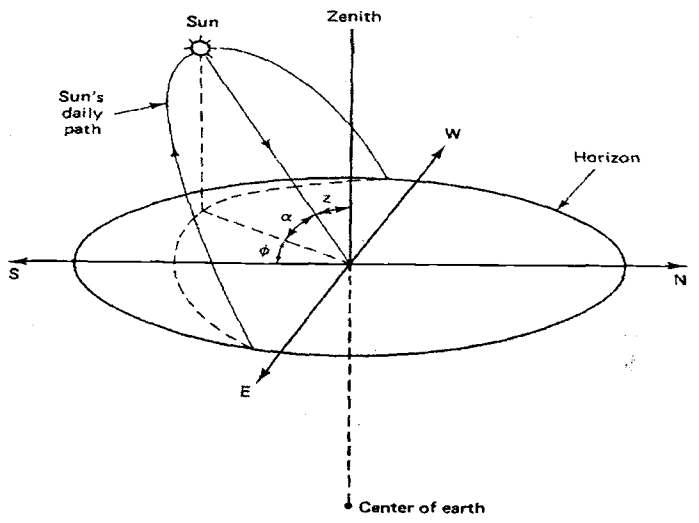

Figure 1B.2 – Derived Solar Angles

α: Solar Altitude z: Zenith Angle ϕ: Solar Azimuth

(Figures from Hsieh 1986 pp 12-14)

A Spatially Explicit Network-Based Model for Estimating Stream Temperature Distribution – Calibration and Sensitivity

Abstract

The WET-Temp (Watershed Evaluation Tool – Temperature) model of stream temperature distribution, described in a companion paper, has been calibrated to a subwatershed of the South Santiam River in western Oregon Cascades. The mean difference between modeled and measured values in McDowell Creek for daily maximum temperature was 0.6°C and for daily minimum temperature was 1.3°C. The parameter set used to calibrate McDowell Creek was used to simulate temperature distribution in an adjacent watershed, and compared with measured results. The mean differences between modeled and measured values in this paired basin were 1.8°C for daily maximum temperatures and 1.4°C for daily minimum temperatures. Sensitivity metrics representing the stream network were developed, and analyses were performed to determine relative sensitivities of model parameters. The results showed that maximum temperatures across the network were most sensitive to the temperatures of incoming flow and channel parameters such as width to depth ratio and reach volume. WET-Temp is useful for the prediction of stream temperature distributions and can serve as a template for future research toward the understanding of stream temperature in the context of stream networks.

Introduction

Anadromous fish stocks have been on the decline in the Pacific Northwest for decades. Nehlsen et al. (1991) reports that hundreds of salmon stocks in the Pacific Northwest were at risk of extirpation and that more than 100 of these stocks have already disappeared. The reasons for this decline are numerous, including hydroelectric dams, over-harvest, and degradation of spawning habitat through various land use activities such as grazing, logging, road building, and mining. These activities can alter stream hydrology and remove riparian vegetation, exposing streams to heightened levels of solar radiation. This radiation is the largest source of energy available to heat streams (Sinokrot and Stefan 1993, Beschta 1997) and consequently drives heat exchange at the stream surface. Concentrations of dissolved oxygen as well as metabolic rates of most aquatic organisms are dictated by water temperature (Hauer and Lamberti 1996; Horne and Goldman, 1994), and stress due to elevated stream temperatures can affect the mortality and life cycles of anadromous fish species (Beschta et al. 1987, Chen 1996). The water quality standard for stream temperature in Oregon is 64°F (17.7°C), and the Oregon Department of Environmental Quality has determined that more streams in the state are water quality limited due to elevated temperature than any other pollutant (Oregon Department of Environmental Quality 1998).

Computer modeling provides a powerful tool to aid in understanding the processes that affect stream temperature. Early models describing the influences of physical processes on stream heating were developed by Beschta and Weatherred (1984), and Theurer (1984). Boyd (1996) built on these models to produce Heat Source, the most recently developed reach scale temperature model. Stream temperature at any single reach is affected by upstream contributions, and Chen et al. (1998) developed watershed scale modeling strategies to account for this fact.

WET-Temp extends these efforts by incorporating spatially distributed datasets into the prediction of temperature distributions across stream networks. Modeled

diurnal fluctuations have been calibrated to three measured sites in McDowell Creek. Results of a simulation in an adjacent watershed (Hamilton Creek), using the same parameter set, are examined to establish model accuracy. Understanding the effects of various heating and cooling processes on stream temperature distributions across networks has been a goal of this research. Sensitivity analyses examining temperature extremes, timing of these extremes, and heating rates across the stream network have been conducted to study the effects of these processes.

The development of WET-Temp was driven by the need for tools to help in the evaluation of restoration strategies at a watershed scale. Beschta et al. (1987) note that once heated in a reach lacking vegetation, a stream will not necessarily cool when reaches with greater shade are encountered below. The stream will tend to stay at the warmer temperature unless mixed with colder water. It follows that stream temperature can be elevated in an additive manner over a network. The same restoration strategy implemented at different sites within a network may produce different results. Modeling stream temperature at the watershed scale will allow for the evaluation of these strategies across entire networks.

Model Description

Representation of the stream network is outline in Figure 2.1. WET-Temp estimates temperature distributions based on the energetic contributions of solar radiation, longwave radiation, evaporation and convection. Advective inputs from in-stream and groundwater flows are also considered, with an assumption of steady and uniform equilibrium flow across each subreach. The sum of these processes is expressed as a differential energy balance and applied at each subnode in the network (Cox, 2002).

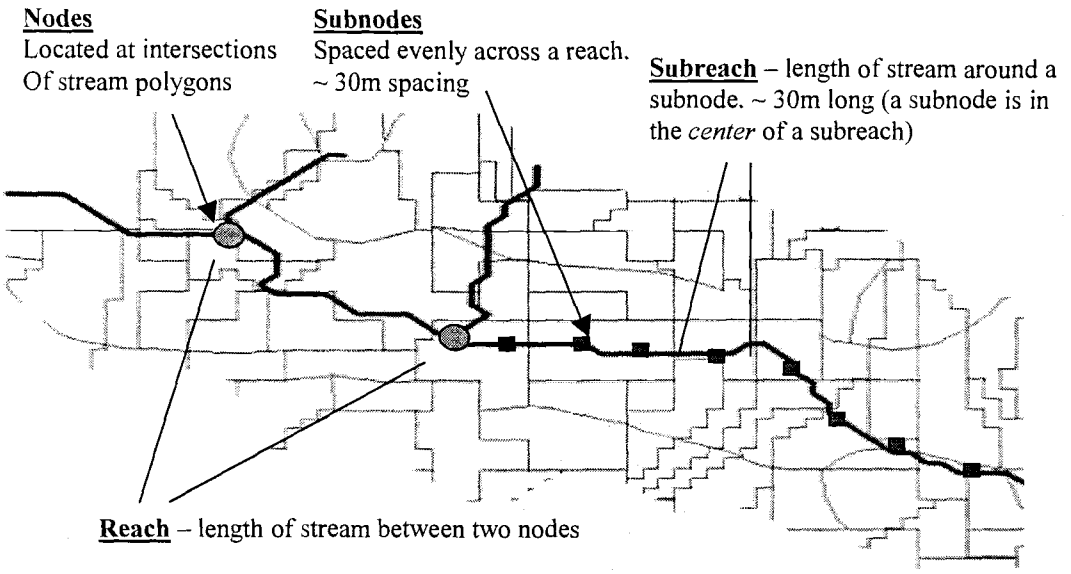

Figure 2.1 – WET-Temp Stream Network Description

Description of Study Area

The South Santiam River, flowing off the western slopes of the Cascade range, is a main tributary of the Willamette River. Two subbasins in the lower part of the basin, McDowell Creek and Hamilton Creek, are the focus of this study (see Figure 3). These subbasins drain approximately 62km^2 (24 mi^2) and 104 km^2 (40 mi^2) respectively. They span from the Willamette Valley Plains ecoregion (67 meters minimum elevation) to the West Cascade Montane Highlands ecoregion (1350 meters maximum elevation). Roughly 80% of these watersheds are made up of steep forested terrain, with the remaining 20% consisting mainly of lower elevation, low gradient agricultural lands (South Santiam Watershed Council and E&S Environmental Chemistry Inc., 1999).

The climate in the basin is Mediterranean in nature, with cool wet winters and warm dry summers. Annual precipitation across the basin varies from 112 cm (44 in) at the valley floor to over 213 cm (84 in) in the higher elevations (Oregon

Climate Service 1990). In the warmest months (July and August), air temperatures fluctuate from lows near 10°C (50°F) to highs near 27°C (80°F). Rain dominates at the low and mid elevations, while persistent snow is present at the high elevations. The system is winter rain dominated, with high flows normally occurring in January or February. Higher elevation streams have generally moderate to high gradients, with conifers and western red alder as common riparian constituents. Many of the low gradient valley streams have been channelized to drain agricultural fields, and their water is heavily withdrawn for irrigation. Riparian vegetation consists of conifers at well drained sites and hardwoods (Oregon ash and western red alder) at poorly drained sites (South Santiam Watershed Council and E&S Environmental Chemistry Inc., 1999).

Ownership in the South Santiam is approximately 30% federal government (BLM and US Forest Service) and 70% private. Private lands consist of both industrial forest land and agricultural land. Watershed council restoration projects will generally involve private lands, so the watersheds chosen for analysis are mainly in private ownership. 85% of the lands in Hamilton Creek and 92% of the lands in McDowell Creek are privately owned.

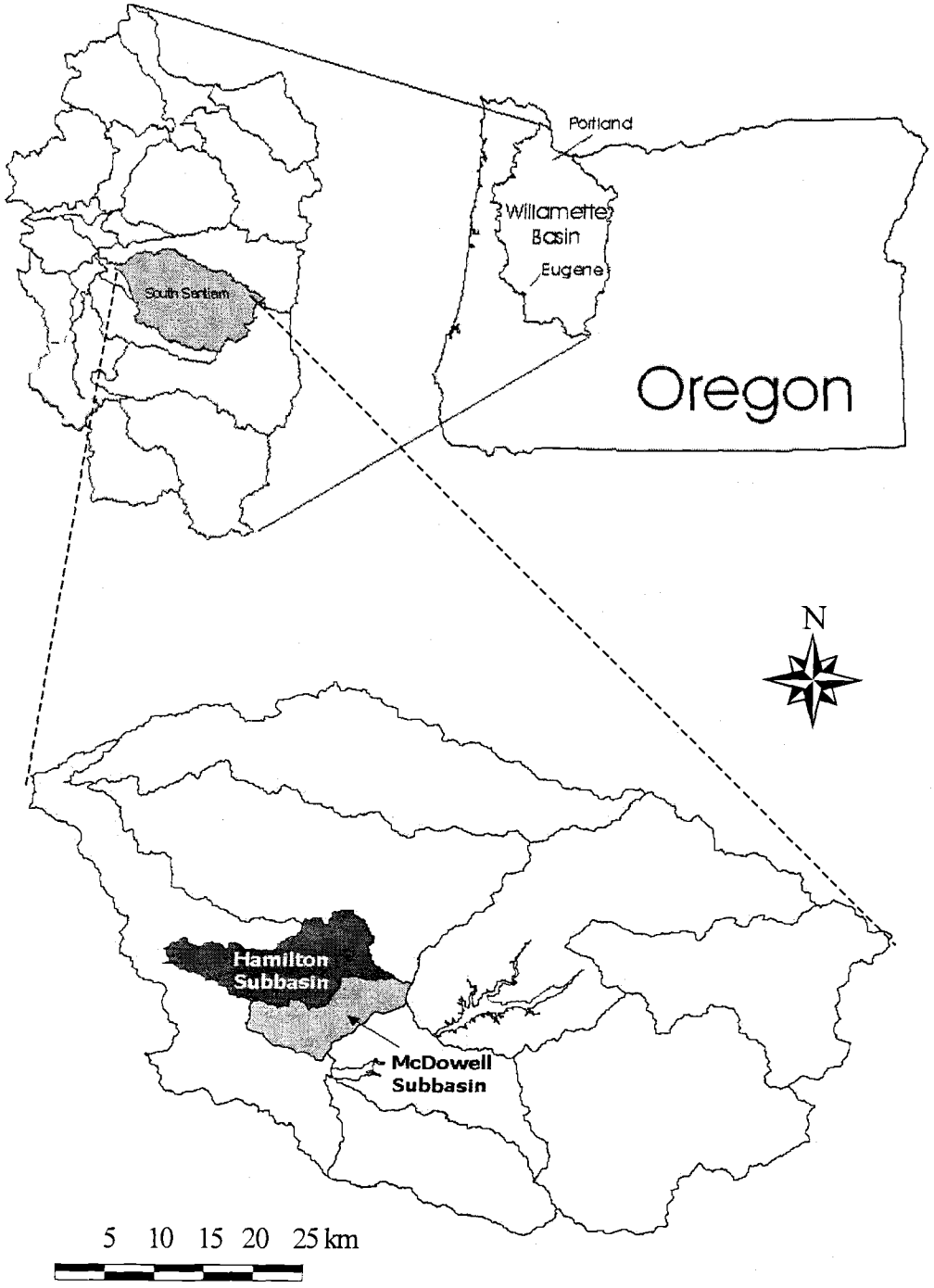

Figure 2.2 - Subbasins of Study within the South Santiam basin, Oregon

Spatial Data

Spatial data layers (in the form of ESRI shapefiles and grid coverages) are utilized to perform temperature analyses with WET-Temp. 10m resolution digital elevation models (USGS) are used to generate stream networks as well as to calculate topographic shading during model preprocessing. A shapefile containing points of known stream discharge (taken in August 2000 and assumed to represent low flow conditions) is used to distribute flow throughout the stream network (Cox, 2002).

WET-Temp utilizes a 30m vegetation grid of land use/land cover classes adapted from Landsat TM satellite images (Oetter et al. 2001). Solar radiation must travel through riparian vegetation before contacting the stream surface in many locations. Information about the structure of riparian vegetation is therefore crucial for the estimation of shortwave solar radiation input to the water column. Timing and magnitude of radiation attenuation by riparian vegetation is dictated by vegetation height and density. Vegetation height and density values are assumed (see Appendix 2C) given vegetation ages and descriptions from the land use/land cover classes. Values used by Ritchey (2000) were taken as a starting point for these assumptions.

Climate Data

Time-series estimates of air temperature, relative humidity and wind speed are required to quantify the influences of evaporation, convection and longwave radiation on the overall energy balance. Continuous relative humidity and air temperature data from the South Santiam were obtained from DEQ field measurements taken at 3 sites from July 25th-27th, 2000. These data were fit with sinusoidal models which are used by WET-Temp as time series estimations of these parameters (See Appendix 2A). Wind speed data from a riparian data station in the western Cascades (but outside of the study subbasins) was utilized (see

Appendix 2B). Diurnal profiles w were similar, so one day was randomly chosen as representative. Evaporation coefficients can be adjusted to allow for changes in wind speed magnitude. Spatial homogeneity of microclimatic variables is assumed in WET-Temp because methods do not currently exist for the describing these variables at the landscape scale (Oregon Department of Environmental Quality, 2001).

Channel Description

Distance from the wetted perimeter of the stream to the nearest riparian vegetation is an important geometric relationship that must be estimated. This non-vegetated area surrounding the stream (including the low-flow channel width) is termed the near stream disturbance zone (*nsdz*). The *nsdz* width is related to bankfull (*bfw*) width and is in general slightly larger. The *nsdz* width is an average of 17% larger than the *bfw* at 24 sites throughout the South Santiam (Figure 2.3). *Bfw* must be estimated for each reach in the network so that we can take advantage of the *bfw/nsdz* relationship. Measured *bfw* values at the 24 sites were linearly regressed against area drained (Figure 2.4), and this relationship is used by WET-Temp to assign each reach a *bfw* value.

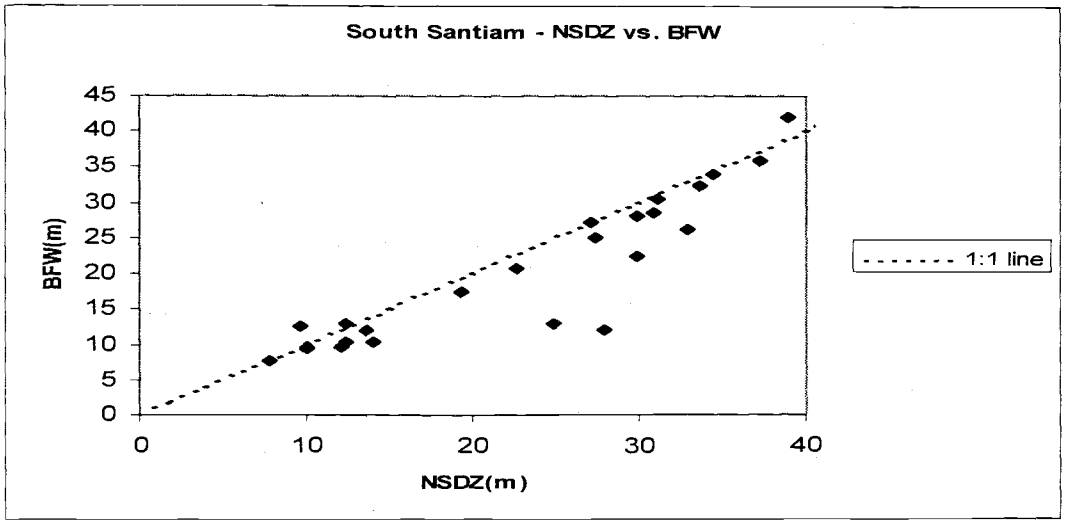

Figure 2.3 – Near Stream Disturbance Zone/Bankfull Width relationships in the South Santiam basin

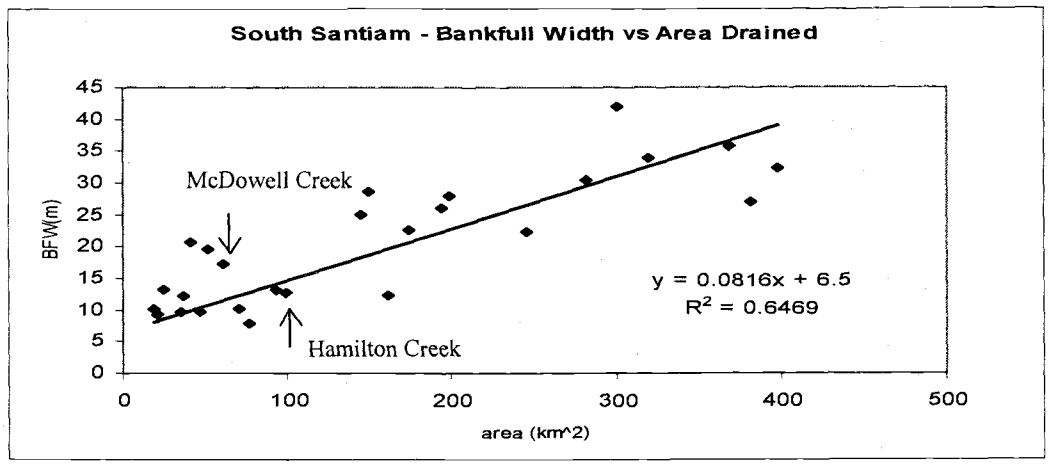

Figure 2.4 - Bankfull Width/Drainage Area Relationships in the South Santiam basin, with data points representing McDowell and Hamilton Creeks identified.

The final step in *nsdz* width estimation is assignment of *nsdz/bfw* relationships based on Rosgen Level 1 (RL1) stream type. RL1 stream types are a useful rough description of general geomorphic characteristics (Rosgen 1996) and are assigned to each reach in our study subbasins using gradient and sinuosity values (Table 2.1). RL1 classes are estimated in Table 2.1 given general type descriptions from Rosgen (1996) and the author's observations of channel structures in these subbasins. Gradient is the elevation difference in a given reach over its length (rise/run). Sinuosity is defined as actual reach length divided by the shortest line between the start and endpoints of the reach. RL1 type A and B streams are usually contained in high gradient, low sinuosity channels. *Nsdz* width should be closer to *bfw* for these highly constrained channel types. Other stream types tend to be more sinuous and are assumed to have larger nsdz widths. Nsdz width is calculated using Eq 2.1 for RL1 A and B stream types, and Eq 2.2 for other stream types.

$$nsdz = bfw + 0.1 * bfw \qquad \text{(Eq 2.1)}$$

$$nsdz = bfw + 0.25 * bfw \qquad \text{(Eq 2.2)}$$

Gradient	< 1.0	< 1.8	< 4.5	< 8.0	< 999
Sinuosity					
< 1.1	F	B	A	A	A
< 1.2	F	G	B	B	A
< 1.4	F	F	F	B	B
< 1.5	C	C	E	B	B
< 999	C	C	E	B	B

Table 2.1 – Estimated Rosgen Level 1 Stream Types for Subbasins of Study

Model Calibration

WET-Temp was calibrated using three continuous temperature data series from McDowell creek. These data, made available by the Oregon Department of Environmental Quality, were collected in the summer of 2000. Model input parameters (Cox, 2002) were adjusted manually until the best fit was obtained, with "best fit" defined as the minimization of the sum of an error statistic (Eq 2.3), calculated at all three sites. The error statistic is an estimate of the area between the measured and modeled temperature curves over the 48-hour time period shown (Figures 2.6 - 2.8). WET-Temp equilibrated quickly on watersheds of the size studied, and two days was determined to be sufficient for model spin-up. Table 2.2 reports the "best fit" parameters obtained during calibration on McDowell Creek. All parameters in Table 2.2 except for groundwater and initial temperature are dimensionless.

$$ErrorStatistic = \sum \left| MeasuredTemp - ModeledTemp \right| \cdot timeStep \qquad \text{(Eq 2.3)}$$

Parameter	"Best Fit" Value
EvapA	0.5
EvapB	0.1
$T_{groundwater}$ (°C)	15
$T_{initial}$ (°C)	15
Manning's n	0.03
Cloud Fraction	0.3
Width/Depth Ratio	55
Volume Multiplier	3
Flow Multiplier	1

Table 2.2 - McDowell Creek "Best Fit" Parameters

Three calibration sites in McDowell Creek were chosen to coincide with available data from the Oregon DEQ (Figure 2.5). Calibration focused on Julian days 208 and 209 (July 27th and 28th) in the summer of 2000 (see Fig 2.6 - 2.8). Energy balance calculations were not performed on reaches with estimated flows less than a cutoff of 0.025 m^3/s (approx. 1 cfs), under the assumption that these reaches have negligible influence on temperature distributions (non-bold, Figure 2.5). Discharge from these reaches was added to downstream reaches at a constant temperature equal to the initial temperature in the network. The mean differences between measured and modeled results were 0.6 °C for daily maximum temperatures and 1.3 °C for daily minimum temperatures (6 observations each, 2 days at 3 sites). Simulated time of maximum temperature values tend to be shifted earlier than measured values at the most upstream site (McDowell Park, Fig 2.6) and shifted later than measured values at the most downstream site (Mouth, Fig 2.8).

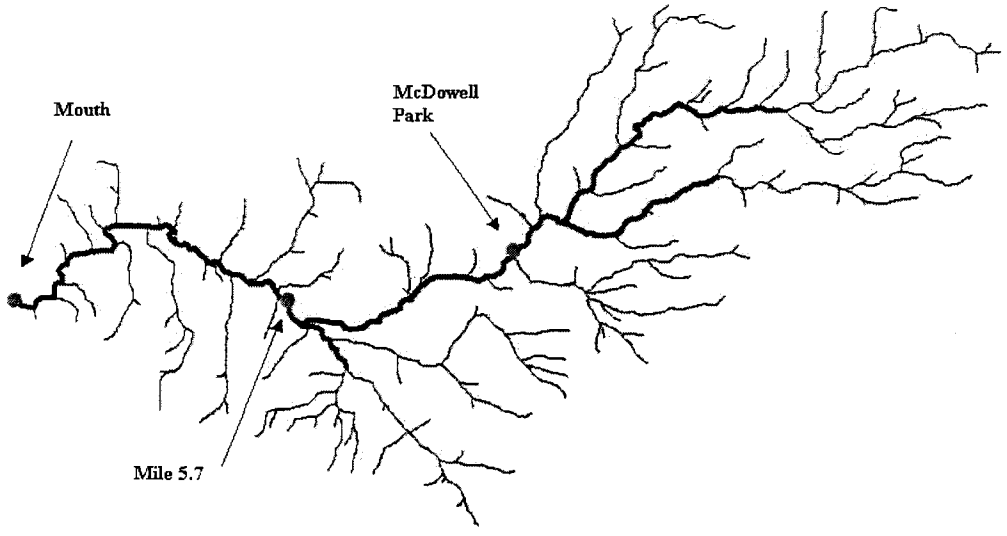

Figure 2.5 - McDowell Creek Calibration Sites

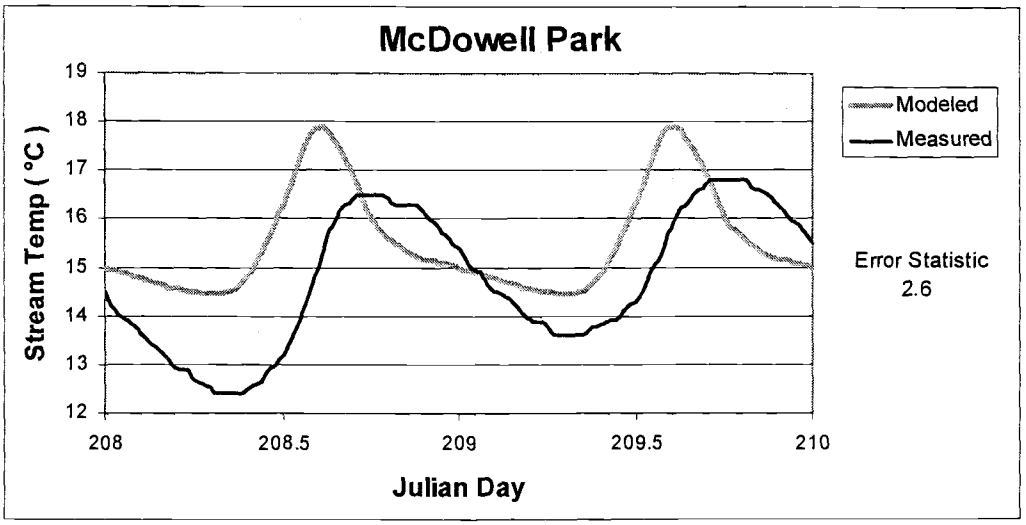

Figure 2.6 – McDowell Park Best Fit Calibration

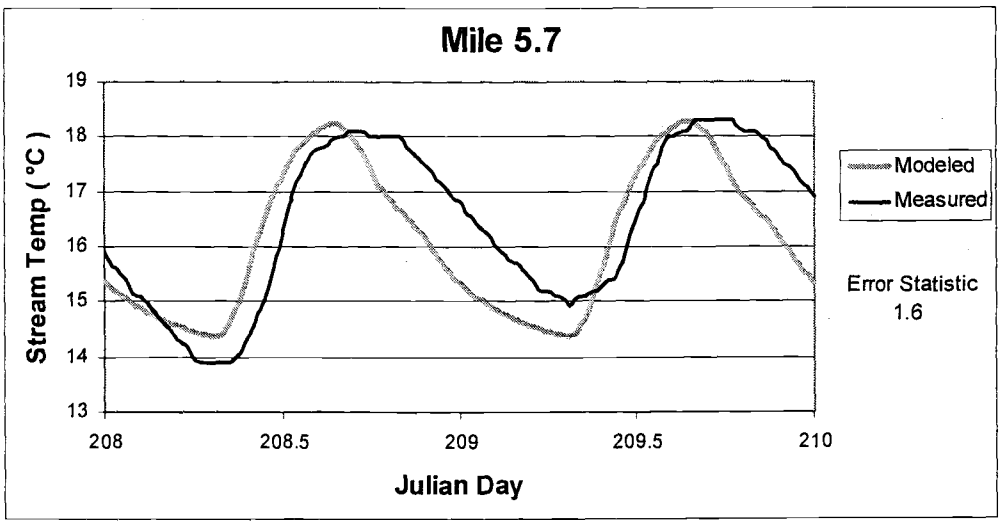

Figure 2.7 – Mile 5.7 Best Fit Calibration

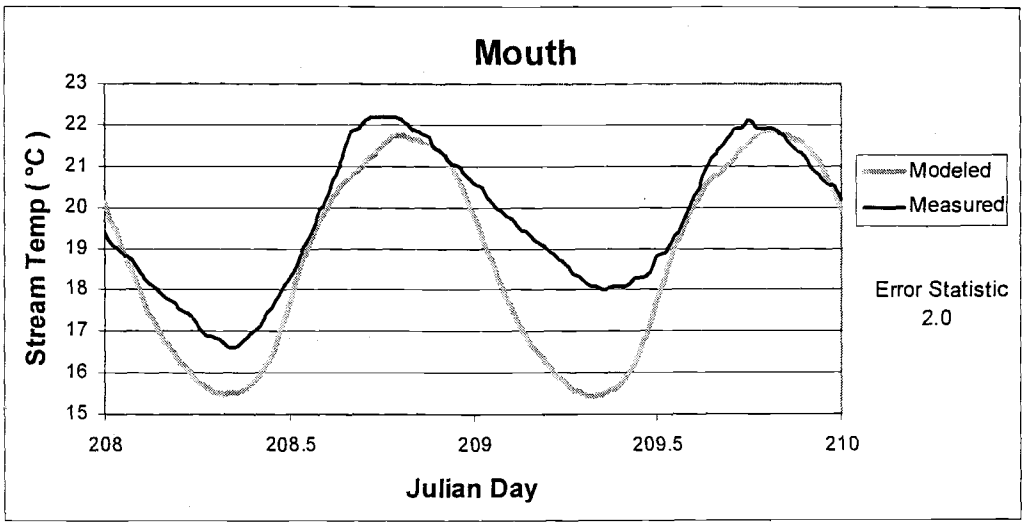

Figure 2.8 – Mouth Best Fit Calibration

The best fit parameters used to calibrate the model to McDowell Creek were used to run a simulation for an adjacent watershed, Hamilton Creek. Hamilton Creek drains almost twice the area of McDowell Creek, but is in many other respects similar. The majority of each watershed is made up of steep, forested terrain, but each becomes a low gradient floodplain system in the lower main stem. The specific discharge (at low flow) in Hamilton Creek (0.12 m^3/km^2) is similar that of McDowell Creek (0.11 m^3/km^2), another signal that these basins are hydrologically similar.

The error statistics were higher on average in Hamilton Creek (7.9) than in McDowell Creek (2.1) using the McDowell Creek best fit parameters. The mean differences between measured and modeled results were 1.8 °C for daily maximum temperatures and 1.4 °C for daily minimum temperatures (8 observations each, 2 days at 4 sites). The location of Hamilton Creek calibration sites (Figure 2.9), the results of the calibration for Julian days 208 and 209 (Fig 2.10 – 2.13), a

longitudinal flow profile (Fig 2.14) and a longitudinal temperature profile at 4:48pm (Fig 2.15) are shown below.

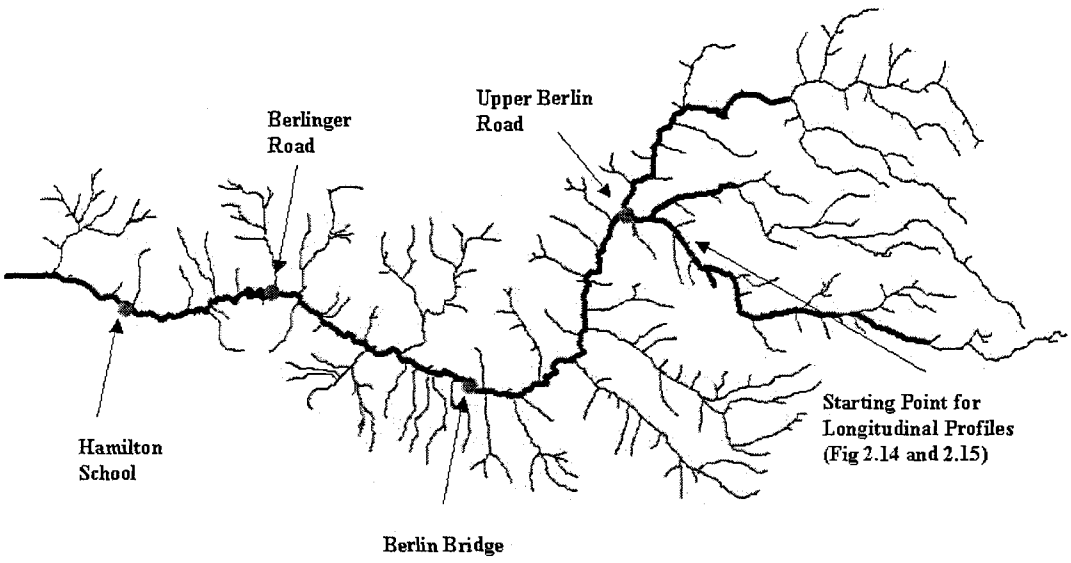

Figure 2.9 – Hamilton Creek Calibration Sites

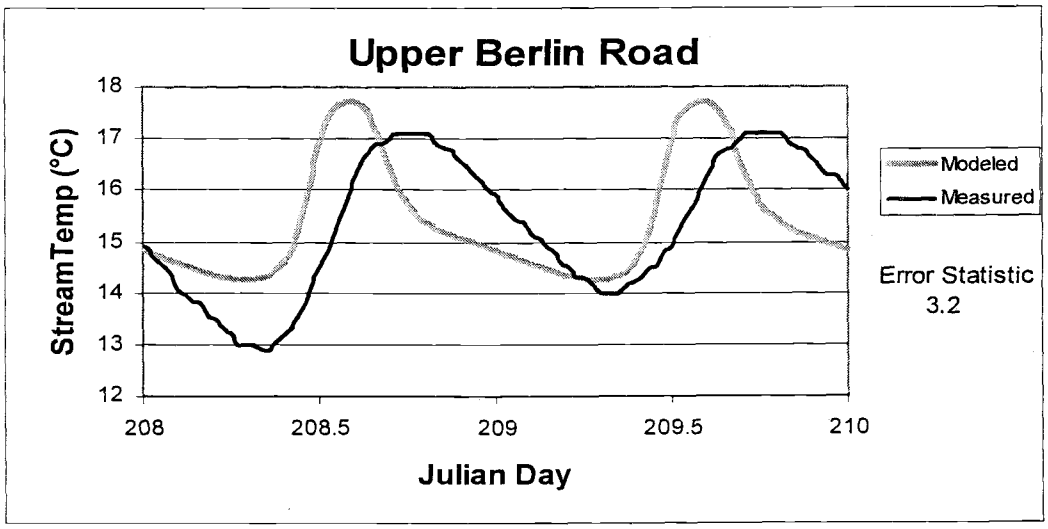

Figure 2.10 – Upper Berlin Road Simulation (Best Fit)

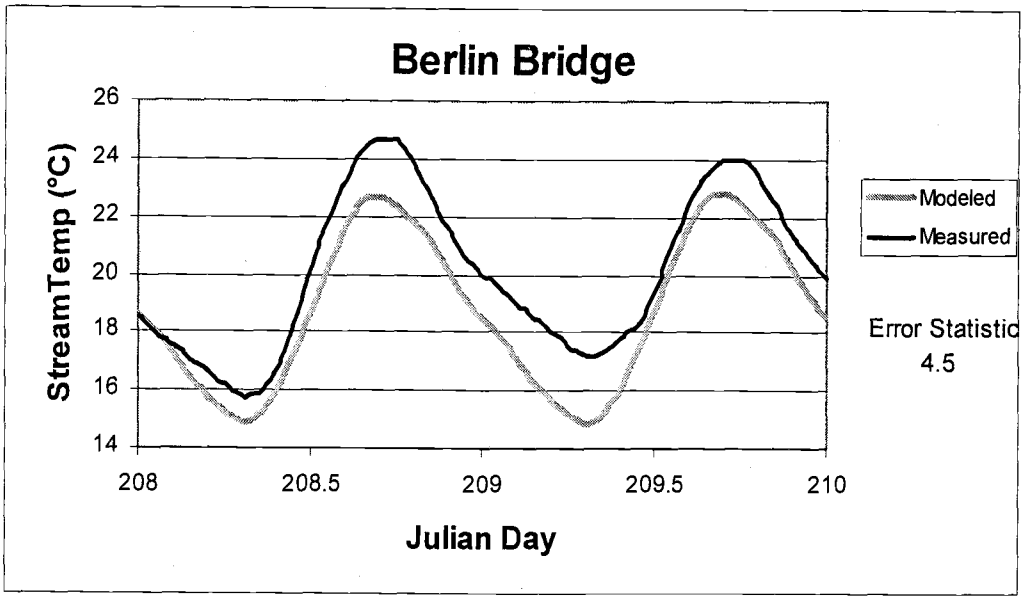

Figure 2.11 – Berlin Bridge Simulation (Best Fit)

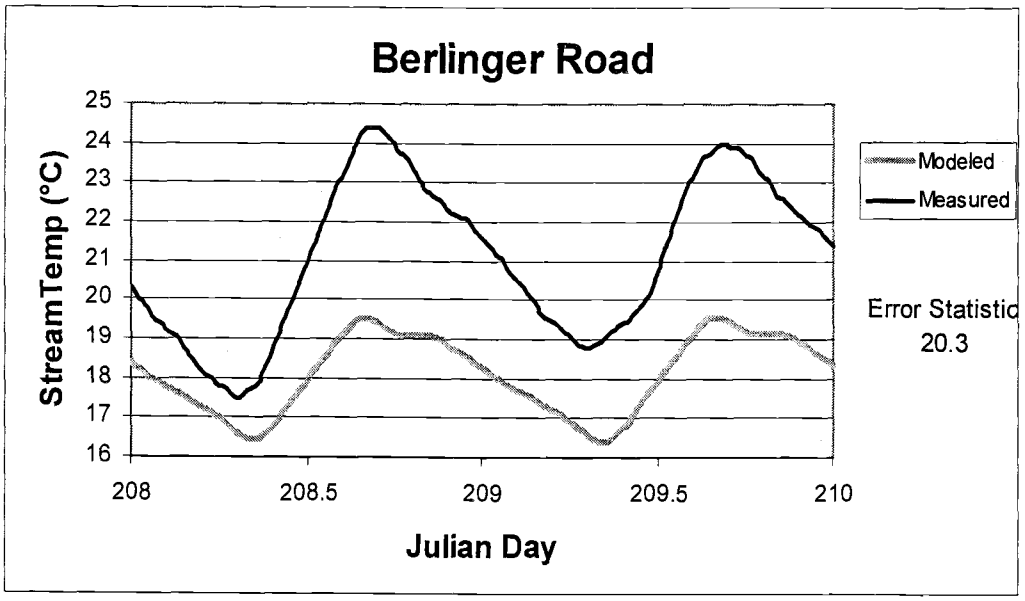

Figure 2.12 – Berlinger Road Simulation (Best Fit)

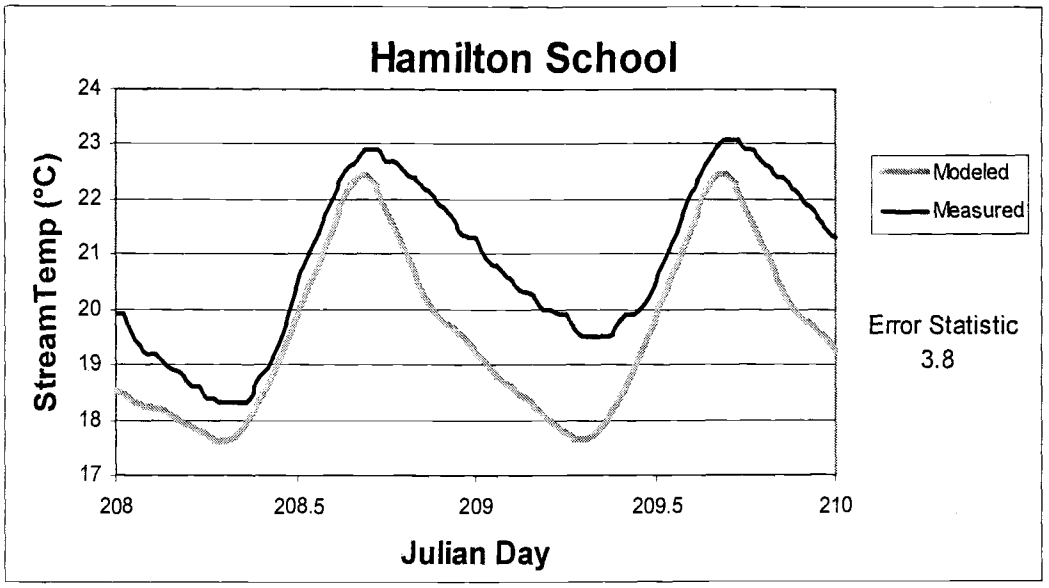

Figure 2.13 – Hamilton School Simulation (Best Fit)

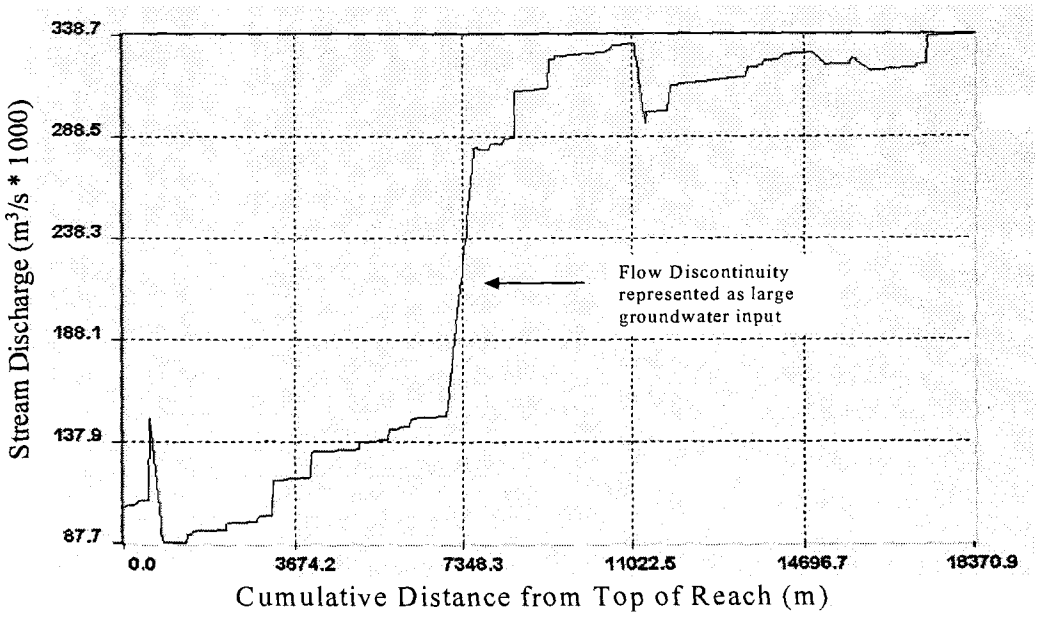

Figure 2.14 – Longitudinal Flow Profile on Hamilton Creek

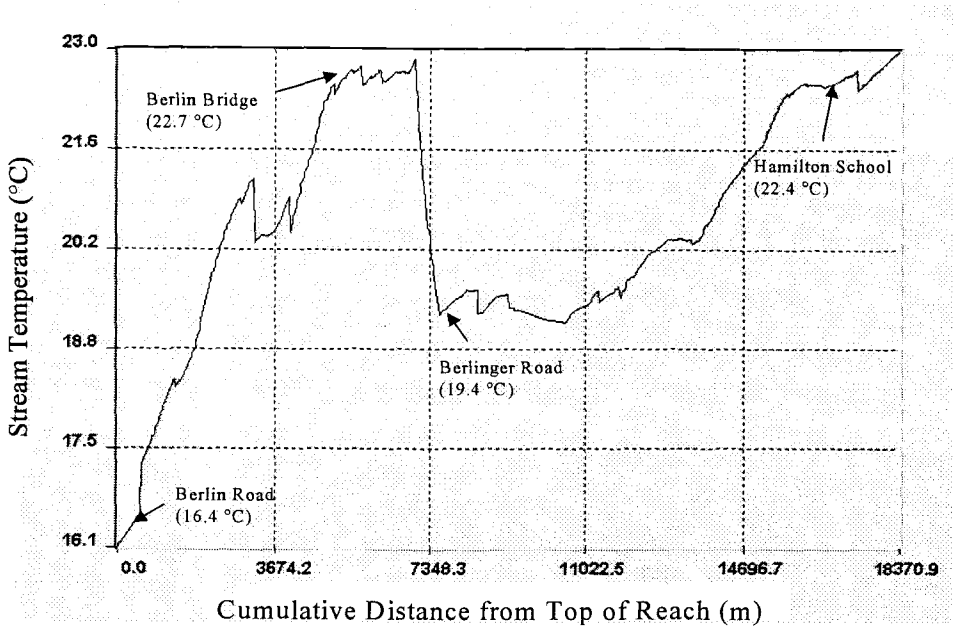

Figure 2.15 – Longitudinal Temperature Profile on Hamilton Creek
[Julian Day = 208, Time of Day = 0.7 (4:48 pm)]

Sensitivity Analysis

Sensitivity analysis is used to examine effects of input parameter perturbations on model output. Sensitivity information gives a measure of the impacts of various model parameters on temperature dynamics, and is useful in understanding modeled relationships and guiding calibration. Output from WET-Temp is not simply temperature at a point, but temperature distribution within a stream network. Appropriate metrics were developed to examine the sensitivity of these distributions to changing model inputs (cloud fraction, groundwater temperature, volume multiplier, etc…).

Diurnal temperature curves have a general sinusoidal shape. Metrics used to examine changes in these curves must address amplitude and phase shift changes.

Maximum and minimum temperatures, the extremes of the diurnal curve, represent the amplitude. The metrics used to describe each of these are simply the change in maximum or minimum temperature averaged over the stream network (T_{max}avg, T_{min}avg). Timing of the maximum and minimum temperatures represents phase shift in the diurnal curve. The metrics describing this shift are changes in the times of these extremes, averaged across the network ($time_{max}$avg, $time_{min}$avg). Sensitivty can be represented in terms of units (i.e. Δ°C per m^3/s discharge) or made dimensionless by standardization (percentages). These are termed absolute and relative sensitivities respectively and are defined for this analysis as follows:

$$S_{Absolute} = \frac{\Delta metric}{\Delta parameter} \qquad \text{(Eq 2.4)}$$

$$S_{Relative} = \frac{\%\Delta metric}{\%\Delta parameter} \qquad \text{(Eq 2.5)}$$

The four metrics mentioned above (T_{max}avg, T_{min}avg, $time_{max}$avg, $time_{min}$avg) describe diurnal dynamics at each reach and, although averaged across the network, are not explicitly representative of network connectivity. The distance metric was formulated to examine the longitudinal gradients of temperature at a point in time. At any particular time (t) the distance metric is defined by the difference between stream temperatures at two points in the network over the distance between these points (Eq 2.6). The comparison between two points along the network allows connectivity to be addressed.

$$\text{DistanceMetric}_t\,(°C/km) = \frac{\text{TempDownstream}_t - \text{TempUpstream}_t}{\text{Distance between points}} \qquad \text{(Eq 2.6)}$$

The following eight tables (Table 2.3 – 2.10) list the results of the sensitivity analysis performed on WET-Temp. Information is grouped by the sign of the

change in the particular metric (- or +) and reported in descending order of $|S_{relative}|$. All parameters shown are dimensionless except for $T_{groundwater}$ and $T_{initial}$. Parameters not included in these tables did not either a) exhibit any sensitivity or b) show a trend when perturbed in a particular direction. The data from which these sensitivity values have been calculated can be found in Appendix 2D.

	ΔParameter	$\|S_{absolute}\|$	$\|S_{relative}\|$
$T_{initial}$ (°C)	+50%	0.765	0.570
$T_{groundwater}$ (°C)	+50%	0.267	0.197
Volume Multiplier	-50%	1.408	0.174
W/D Ratio	+50%	0.030	0.118
Cloud Fraction	-50%	7.400	0.037
EvapA	-50%	0.560	0.024
Flow Multiplier	-50%	0.440	0.022
Manning's n	+50%	8.667	0.013
EvapB	-50%	0.200	0.001

Table 2.3 – Sensitivity of WET-Temp to parameter perturbations causing an increase in the maximum temperature metric ($+\Delta T_{max}avg$)

	ΔParameter	$\|S_{absolute}\|$	$\|S_{relative}\|$
$T_{initial}$ (°C)	-50%	0.564	0.597
$T_{groundwater}$ (°C)	-50%	0.268	0.284
W/D Ratio	-50%	0.037	0.145
Volume Multiplier	+50%	0.656	0.081
Cloud Fraction	+50%	7.400	0.037
EvapA	+50%	0.520	0.013
Manning's n	-50%	8.000	0.012
Flow Multiplier	+50%	0.100	0.005
EvapB	+50%	0.200	0.001

Table 2.4 – Sensitivity of WET-Temp to parameter perturbations causing a decrease in the maximum temperature metric ($-\Delta T_{max}avg$)

	ΔParameter	$\lvert S_{absolute} \rvert$	$\lvert S_{relative} \rvert$
Volume Multiplier	+50%	0.56	0.058
Manning's n	+50%	33.333	0.042
W/D Ratio	+50%	0.009	0.031
Flow Multiplier	-50%	0.740	0.031

Table 2.5 – Sensitivity of WET-Temp to parameter perturbations causing an increase in the time of maximum temperature metric (+ $\Delta time_{max}avg$)

	ΔParameter	$\lvert S_{absolute} \rvert$	$\lvert S_{relative} \rvert$
Volume Multiplier	-50%	0.72	0.075
Manning's n	-50%	39.333	0.049
Flow Multiplier	+50%	0.740	0.031

Table 2.6 – Sensitivity of WET-Temp to parameter perturbations causing a decrease in the time of maximum temperature metric (- $\Delta time_{max}avg$)

	ΔParameter	$\lvert S_{absolute} \rvert$	$\lvert S_{relative} \rvert$
$T_{initial}$ (°C)	+50%	0.767	0.811
$T_{groundwater}$ (°C)	+50%	0.268	0.283
Flow Multiplier	-50%	1.140	0.080
Manning's n	+50%	24.000	0.051
Volume Multiplier	+50%	0.288	0.051
W/D Ratio	+50%	0.006	0.032
EvapA	-50%	0.280	0.010
Cloud Fraction	-50%	0.400	0.003
EvapB	-50%	0.100	0.001

Table 2.7 – Sensitivity of WET-Temp to parameter perturbations causing an increase in the minimum temperature metric ($+\Delta T_{min}avg$)

	ΔParameter	$\|S_{absolute}\|$	$\|S_{relative}\|$
$T_{initial}$ (°C)	-50%	0.669	0.709
$T_{groundwater}$ (°C)	-50%	0.174	0.184
Volume Multiplier	-50%	0.744	0.131
Manning's n	-50%	52.000	0.110
Flow Multiplier	+50%	0.960	0.068
W/D Ratio	-50%	0.011	0.064
EvapA	+50%	0.280	0.010
Cloud Fraction	+100%	0.200	0.001
EvapB	+100%	0.100	0.001

Table 2.8 – Sensitivity of WET-Temp to parameter perturbations causing a decrease in the minimum temperature metric ($-\Delta T_{min}avg$)

	ΔParameter	$\|S_{absolute}\|$	$\|S_{relative}\|$
Volume Multiplier	+50%	0.096	0.010
Manning's n	+50%	4.000	0.005
Cloud Fraction	+100%	1.200	0.003
EvapA	+50%	0.080	0.002

Table 2.9 – Sensitivity of WET-Temp to parameter perturbations causing an increase in the time of minimum temperature metric ($+\Delta time_{min}avg$)

	ΔParameter	$\|S_{absolute}\|$	$\|S_{relative}\|$
Volume Multiplier	-50%	0.544	0.057
Manning's n	-50%	29.333	0.037
EvapA	-50%	0.360	0.008
Cloud Fraction	-50%	0.400	0.002

Table 2.10 – Sensitivity of WET-Temp to parameter perturbations causing a decrease in the time of minimum temperature metric ($-\Delta time_{min}avg$)

The distance metric describes the longitudinal heating profile across the network over time. It can be thought of as the "heating trajectory" between two points. Its value would be zero if temperatures at the two points were the same at a point in time. The distance metric is most conveniently displayed as a time series. The same error statistic used in calibration was used as a sensitivity metric for distance. It is an approximation of the area between the distance metric curves. Distance metric sensitivity values are reported in Tables 2.11 and 2.12. Heating in these tables refers to the period when solar radiation is incident on the stream surface, while cooling refers to the periods of no incident solar radiation.

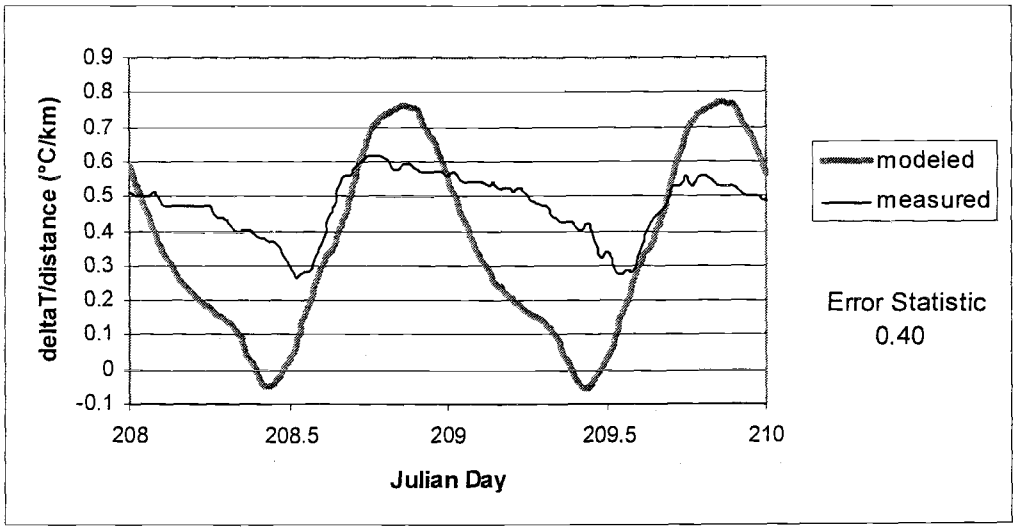

Figure 2.16 - Diurnal fluctuation of distance metric comparing Mile 5.7 and Mouth

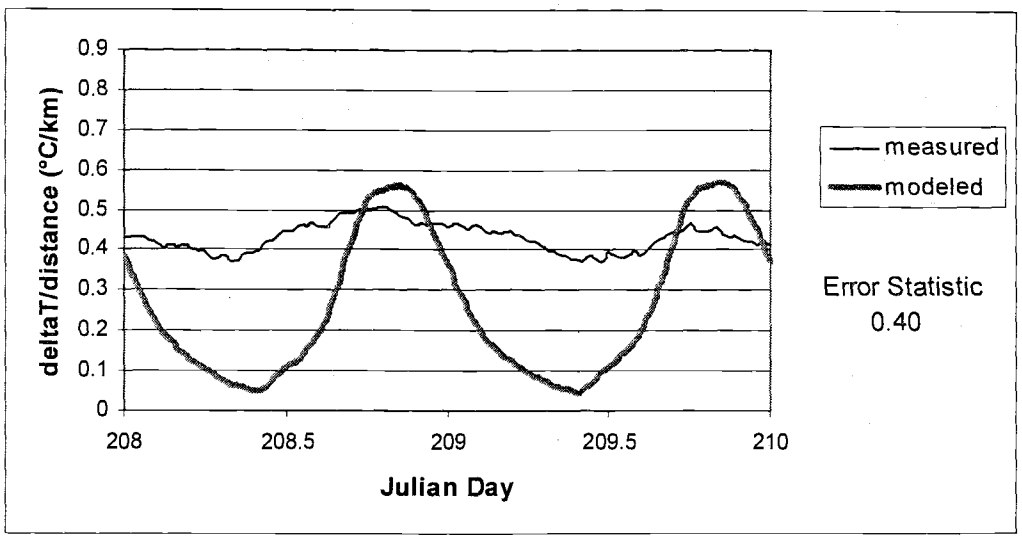

Figure 2.17 - Diurnal fluctuation of distance metric comparing McDowell Creek Park and Mouth

		Mile 5.7		McDowell Park	
	ΔParameter	Heating	Cooling	Heating	Cooling
Volume Multiplier	-50%	0.080	0.031	0.056	0.010
Flow Multiplier	-50%	0.014	0.014	0.009	0.005
Manning's n	+50%	0.009	0.009	0.006	0.004
W/D Ratio	+50%	0.003	0.004	0.020	0.015
$T_{initial}$ (°C)	+50%	0.003	0.003	0.001	0.001
$T_{groundwater}$ (°C)	+50%	0.001	0.001	0.003	0.003
Cloud Fraction	-50%	0.000	0.001	0.000	0.000
EvapB	-50%	0.000	0.000	0.000	0.000
EvapA	-50%	0.000	0.000	0.000	0.000

Table 2.11 - Distance metric error statistics - parameter perturbations that cause an increase in the maximum temperature metric ($+\Delta T_{min}avg$)

		Mile 5.7		McDowell Park	
	ΔParameter	Heating	Cooling	Heating	Cooling
Manning's n	-50%	0.03	0.02	0.02	0.01
Flow Multiplier	+50%	0.011	0.008	0.009	0.003
Volume Multiplier	+50%	0.007	0.016	0.005	0.007
W/D Ratio	-50%	0.007	0.010	0.003	0.007
$T_{initial}$ (°C)	-50%	0.003	0.003	0.001	0.001
$T_{groundwater}$ (°C)	-50%	0.001	0.001	0.003	0.003
Cloud Fraction	+50%	0.00	0.00	0.00	0.00
EvapA	+50%	0.00	0.00	0.00	0.00
EvapB	+50%	0.00	0.00	0.00	0.00

Table 2.12 - Distance metric error statistics - parameter perturbations that cause an decrease in the maximum temperature metric ($-\Delta T_{min}avg$)

Discussion

Calibration data show that WET-Temp is predicting maximum and minimum temperatures fairly well on Julian days 208 and 209 in McDowell Creek. Spatial representation of the landscape combined with simultaneous solution of energy balances across the stream network has allowed for the accurate representation of temperature distributions. These results point to the potential usefulness of the model for further prediction of maximum daily temperatures.

Predicted diurnal curves for McDowell Creek are in general correct although differences can be observed, especially at times of rapid heating and cooling. These errors are exacerbated as one moves upstream in the network. Comparing Figures 2.6(upstream) and 2.7(downstream) we see that while the magnitudes are reasonable, the rates of heating and cooling in the upstream reach are accelerated. A possible explanation is that the flow prediction method used by WET-Temp (Cox, 2002) assigns higher velocities to streams with higher gradients (generally streams higher in the watershed). This seems reasonable, but the net effect on the

energy balance is that a parcel of water moves more quickly downstream, resulting in loss of energy from the subreach by advection. One explanation might be that streams of higher order may not lose elevation as steadily as assumed in WET-Temp, but in series of steps and pools. The net effect would be lower velocities than modeled, and a slower loss of energy from the subreach through advection. The volume multiplier is a calibration parameter allowing the user to augment the volume of water residing in each subreach. It was added to the model as a way to simulate these steps and pools, but it is applied across the network evenly. An improved representation of the movement of water through the system would vary this multiplier based on geomorphic characteristics of each reach.

Model calibration opens up the possibility of misrepresentation of some heat flux processes. Parameters governing processes such as evaporation and groundwater interactions may affect the diurnal temperature curve similarly. It follows that an overestimation of one parameter could be compensated by an underestimation of the other. This could happen for parameters governing heating processes and "buffering" processes as well.

Sinuosity is estimated from the DEM generated stream coverage. This method may underestimate micro-scale sinuosity in places, particularly low gradient areas. Circumstantial evidence for this is that the "Mile 5.7" study site is only 4.2 miles from the mouth of our DEM generated stream network. This underestimation has the potential to affect the residence time of water in the landscape, and therefore stream temperature distributions across the network.

Examination of the measured versus modeled distance metric between Mile 5.7 and the Mouth (Figure 2.16) shows that while the general shape of the curve is good (similar inflection points), the model misses on the longitudinal trajectory over much of the diurnal cycle. The modeled distance metric in the late evening it is too high, signifying an overestimation of the "heating trajectory". This stems from the fact that timing of the daily maximum at the mouth is late and cooling is delayed. A few hours prior midnight, we are overestimating temperature at the

mouth while underestimating at Mile 5.7, leading to a high longitudinal trajectory. From midnight until noon the model underestimates "heating trajectory". This stems from an underestimation of temperature at the Mouth combined with an overestimation at Mile 5.7. The model adequately represents the timing of the distance metric's maximum and minimum at Mile 5.7, although the values are slightly shifted. The distance metric is not modeled accurately at McDowell Park (Figure 2.17). This is not surprising when we examine Figure 2.6 and notice that at any single point during the diurnal cycle, the modeled and measured temperatures are disparate. The intersections of measured and modeled curves for both temperature and distance metric occur simultaneously as would be expected. Further calibration of the model to match the distance metric would be facilitated by the ability to calibrate sections of the watershed (i.e. the lower reaches and headwaters) separately based on their respective characteristics.

Figure 2.16 illustrates an interesting phenomenon observed in McDowell Creek. In the measured data, the temperature difference between the two points rises sharply around mid afternoon (when temperatures are at their maximums). This difference gradually gets smaller throughout the night. This implies that McDowell Creek is heating more rapidly at its mouth than at the Mile 5.7 data collection site. The diurnal changes in the distance metric at McDowell Park (Figure 2.17) are less pronounced, possibly due to the greater distance between the two points.

WET-Temp is extremely sensitive to initial temperature ($T_{initial}$) and groundwater temperature ($T_{groundwater}$). $T_{initial}$ represents the upstream boundary condition as modeled, and is the most influential parameter. The magnitude of this influence would likely change if the flow cutoff is adjusted so that energy balances are calculated at more subnodes (and less flow enters the network at $T_{initial}$). In this study, water is constantly being input to the system at $T_{groundwater}$, making it very influential. Its effect is equally strong on both daily minimums and maximums. As

modeled, $T_{groundwater}$ does not take into account local effects, which are known to be of ecological importance (Torgersen et al. 1999).

The strong influence of width to depth ratio (W/D ratio) on maximum temperature increase and decrease is not surprising. Increasing the W/D ratio for a given flow rate increases the surface area subject to heat flux processes, namely solar radiation. For a given volume of water, increasing W/D ratio reduces the depth of the stream. Minimum temperatures are also affected by W/D ratio, but much less so. This may be an artifact of the effect of increased maximum temperatures (higher maximums can potentially lead to higher minimums). The distance metric is slightly affected by W/D ratio at mile 5.7 and more strongly affected at McDowell Park. This may be a response to lower overall flows at McDowell Park.

The volume multiplier has a very strong influence on both maximum and minimum temperatures. Equivalent amounts of energy imparted on larger volumes (i.e. greater depths) will result in smaller temperature fluctuations. The volume multiplier serves as a "buffering" factor from both positive and negative heat flux. It also exerts the greatest influence of any model parameter on timing of minimum and maximum temperatures. Increasing volumes mean less water flowing out of a subreach (percentage wise), and more energy retained upstream. This effectively delays the timing of the maximum or minimum temperature. The distance metric was strongly affected by decreasing the volume multiplier but only slightly affected by increasing it, suggesting an upper bound in sensitivity to this parameter. The heating periods were most influenced by a decreasing volume multiplier, presumably because its affect on increasing maximum temperature is three times as great as its affect on increasing minimum temperature (see Tables 2.3 and 2.7).

Manning's n has noticeable influence on minimum temperatures as well as timing of maximum and minimum temperatures. This parameter represents surface and form roughness, and water flowing over a rougher surface will flow more slowly, delaying water and the energy associated with it as it moves downstream.

It is noted however that this parameter cannot reasonably be altered a great deal. The value at –50% (0.15) is acceptable only for concrete channels and the value at +50% (0.45) is applicable only to vegetated floodplains (Chanson 1999).

The influence of the evaporation coefficients (EvapA and EvapB) is small. It should be noted however that their "best fit" values are much lower than those reported by Bowie for the San Diego Aqueduct (Bowie 1985). These empirical parameters can be reasonably adjusted much more than 50% in order to capture the magnitude of evaporative fluxes taking place.

Maximum temperatures are moderately sensitive to cloud fraction, which is modeled as a percentage by which total solar radiation is reduced. Cloud fraction is also involved in longwave radiation calculations, although its net affect there is very slight. Timing of maximum and minimum temperatures and the distance metric are not influenced by this parameter.

In shallow streams, solar radiation can be transferred directly to the bed material. If this material is smaller than 25 cm in diameter, the energy is returned immediately back to the water column. For larger diameter substrates this energy can be stored and released over time. Release of this energy is dependent of the size of the substrate and driven by a heat gradient between the water column and bed surface, with net solar energy generally conserved over a diurnal cycle. Bed conduction flux is not considered by WET-Temp due to the difficulty in estimating bed material properties at the landscape scale. It is most likely of greater importance in shallow headwater streams, and could become an important process to consider if the flow cutoff is decreased and energy balances are calculated on smaller streams.

The effect of the flow multiplier on maximum temperature is not as strong as might be expected. This is likely due to fact that the volume multiplier is already in place so that, percentage wise, flow increases do not have such marked increases on subreach volumes. Minimum temperatures are affected more strongly. Lower flow tends to delay the time of daily maximum, as energy is more slowly transferred

downstream. The affect on distance metric, while not large, is more significant than for most parameters. This parameter is envisioned as a tool for analysis scenarios where effective flow is increased or decreased by a certain percentage.

"Best Fit" parameters obtained from hand calibration on McDowell Creek produced reasonably similar results in Hamilton Creek, an adjacent basin (see Figs 2.10 - 2.13). This is likely in part due to geomorphic similarities between the adjacent basins. The error statistics were greater overall for the Hamilton Creek simulation. This should be expected simply because of the multitude of potential differences in basin hydrology (hyporheic connectivity, width/depth ratios etc...). The fact that Hamilton Creek drains nearly twice as much land area as McDowell Creek could result in errors, because the effects of basin size on WET-Temp simulation results has not been tested.

WET-Temp distributes discharge upstream based on a specific discharge calculated at a downstream measurement. This continues until flow is distributed to all the branches of the watershed or until another flow observation is encountered. At this point, the specific discharge is recalculated (Cox, 2002). This abrupt change can cause a flow discontinuity, which can lead to discontinuities in the longitudinal temperature profile. The main reason for underestimation at three sample points on Hamilton Creek (Fig 2.10 – 2.13) has to do with a large flow discontinuity (Fig 2.14). In this case, the result of the discontinuity is a massive influx of groundwater distributed over a single reach. The net effect of this groundwater is to drop the temperature 4 degrees abruptly (Fig 2.15). Further effects of these discontinuities on can be seen on maximum temperatures in McDowell Creek (see Appendix 2E).

Representing the movement of water and the energy it contains is a crux of modeling temperature distribution across stream networks. Generalizations across reaches differing in channel type and structure may lead to inaccurate descriptions of this movement. WET-Temp is highly sensitive to parameters used to describe water movement (W/D ratio, manning's n, volume multiplier), the energy of water

inputs ($T_{groundwater}$, $T_{initial}$), as well as discontinuities in the representation of stream discharge.

Conclusions

Stream temperature is a phenomenon driven by a variety of factors, and predicting its distribution across a spatially and temporally variable stream network is a challenge. As technology advances and richer spatial datasets become available, development of tools to utilize these data is an important endeavor. WET-Temp provides a framework for utilization of spatially explicit datasets, and has the potential to be a useful tool for evaluation of restoration strategies.

WET-Temp successfully modeled maximum stream temperatures (within a mean difference of 0.6 °C) when calibrated to McDowell Creek. Maximum stream temperature is a regulatory standard, and WET-Temp should prove useful in studies focused on regulatory concerns. Because it is a process level, physically based model, WET-Temp should be useful for examining the effects of potential changes in riparian vegetation, in the context of stream restoration, on stream temperature distributions.

Examination of temperature distribution across stream networks, as a connective phenomenon as opposed to a reach scale phenomenon, can shed light on how networks respond to perturbations in their energetic environment. Many difficulties exist when attempting to model these networks. Adequate descriptions of the physical landscape, especially channel structure and hydrology, need to be addressed more completely. Calibrations within the basin of study are necessary at this point to ensure confidence in the results of analyses within that basin.

WET-Temp provides a platform for the incorporation of spatially explicit data into stream temperature analyses. It does not replace existing reach scale models, but instead is able to answer questions related to stream network connectivity and cumulative effects of energy sources and sinks. The use of WET-Temp in

conjunction with reach scale analyses could potentially provide valuable insight into the factors driving observed stream temperature distributions at various scales, and provide solid support for the evaluation of management decisions.

Recommendations for Future Research

WET-Temp should be tested in the future on watersheds outside of the western Cascades to aid in understanding of its strengths and weaknesses as well as for comparison of stream temperature network properties across geologic and climatic regions. Incorporation of day-to-day climate variability will allow simulations of longer duration and insight into the seasonal drivers of stream temperature distributions.

Simulations on a small, well-characterized watershed could provide insight into the small-scale hydrologic processes and geomorphic changes that affect temperature distributions. This information could then be used to associate channel characteristics such a W/D ratio and manning's n with local geomorphology to capture variability across the watershed. Detailed field data on these channel characteristics would remove a great deal of empiricism from the model. Calibration of longitudinal temperature profiles to FLIR imagery could be very helpful in examining the performance of WET-Temp.

References

Beschta, R.L. and J. Weatherred. 1984. A computer model for predicting stream temperatures resulting from the management of streamside vegetation. *USDA Forest Service.* WSDG-AD-00009.

Beschta, R.L. 1997. Riparian Shade and Stream Temperature: An Alternative Perspective. *Rangelands* 19(2): 25-28.

Bowie, G.L., Mills, W.B., Porcella, D.B., Campbell, C.L., Pagenkopf, J.R., Rupp, G.L., Johnson, K.M., Chan, P.W., and S.A. Gherini. 1985. Rates, Constants, and Kinetics Formulations in Surface Quality Modelling, 2nd Edition. EPA/600/3-85/040, U.S. Environmental Protection Agency, Athens, GA.

Boyd, M. 1996. Heat Source : Stream, River and Open Channel Temperature Prediction. Master's thesis at Oregon State University, Department of Bioresource Engineering/Civil Engineering.

Chen, Y.D. 1996. Hydrologic and water quality modeling for aquatic ecosystem protection and restoration in forest watersheds: a case study of stream temperature in the Upper Grande Ronde River, Oregon. PhD dissertation, University of Georgia, Athens, Ga.

Chen, Y.D., R.F. Carsel, S.C. McCutcheon, and W.L. Nutter. 1998. Stream Temperature Simulation of Forested Riparian Areas: I. Watershed-Scale Model Development. Journal of Environmental Engineering 124(4) : 304-315.

Chen, Y.D., S.C. McCutcheon, D.J. Norton and W.L. Nutter. 1998. Stream Temperature Simulation of Forested Riparian Areas : II. Model Application. Journal of Environmental Engineering 124(4) : 316-328.

Cox, M.M. 2002. A spatially-distributed network-based model for estimating stream temperature distribution. Master's Thesis, Oregon State University, Corvallis, OR.

Chanson, H. 1999. The Hydraulics of Open Channel Flow. Arnold, London, 495pp.

Nehlsen W., Williams, J.E. and J.A. Lichatowich. 1991. Pacific Salmon at the Crossroads: Stocks at Risk from California, Oregon, Idaho and Washington. *Fisheries* 16(2): 4-19.

Oetter, D. R., Cohen, W. B., Berterretche, M., Maiersperger, T. K., and R.E Kennedy. 2001. Land cover mapping in an agricultural setting using multi-seasonal Thematic Mapper data. *Remote Sensing of Environment* 76(2): 139-155.

Oregon Department of Environmental Quality. 2001. Upper Klamath Lake Drainage Total Maximum Daily Load (TMDL). Draft report.
Oregon Climate Service. 1990. Zone 2 Climate Data Archives – Foster Dam – Monthly means and extremes (1961-1990). Retrieved on March 26, 2002 from http://www.ocs.orst.edu/pub_ftp/climate_data/mme/mme3047.html.

Ritchey, D. 2000. Design and Prioritized Implementation of Woody Riparian Buffers for Increasing Effective Shade in Agricultural Landscapes of the Willamette River Valley, Oregon. Masters Project. University of Oregon, Eugene, OR.

Rosgen, D. 1996. Applied River Morphology. Wildland Hydrology, Pagosa Springs, CO.

South Santiam Waterhsed Council and E&S Environmental Chemistry Inc. 1999. South Santiam Watershed Assessment. Draft Final Report.

Togersen, C.E., D.M. Price, H.W. Li, and B.A. McIntosh. Multiscale Thermal Refugia and Stream Habitat Associations of Chinook Salmon in Northeastern Oregon. *Ecological Applications*, 9(1): 301-319.

Theurer, F.D., K.A. Voos, and W.J. Miller. 1984. Instream Water Temperature Model. Instream Flow Information Paper 16. *U.S. Fish and Wildlife Service*. FWS/OBS-84/15. 200 pp.

Appendices

Appendix 2A – Air Temperature and Relative Humidity Regressions

Time-series temperature and humidity data was taken from July 25th-27th, 2000. These data were taken at 3 riparian sites in the basin:

- South Santiam main stem (elevation 82m)
- Hamilton Creek (elevation 187m)
- Crabtree Creek (elevation 466m)

Time series air temperature data from the 25th were fit with a sinusoidal model in the form of:

$$a + b \cdot \sin(T \cdot \left(\frac{2\Pi}{24}\right) + c) \qquad \text{(Eq 2A.1)}$$

where,

T = time (hour, between 0 and 24)

a,b,c = model parameters

A fourth parameter correlating the sites with elevation was used initially, but model fit was found to be better when it was excluded. Total mean square error between modeled and measured values for the 3 sites was minimized to obtain the parameters used by WET-Temp. A graphical representation of the model fit is shown in Figure 2A-1. The results of this model were compared against the data from July 26th and 27th, 2000 (Figures 2A.2, 2A.3). Although there was less agreement with the data on the 26th and 27th, the model fit was assumed to be acceptable for our purposes. An identical procedure was used to estimate values of relative humidity. A sinusoidal model was fit to the data from the 25th (Figure 2A.4) and then compared to data from the 26th and 27th (Figure 2A.5, 2A.6).

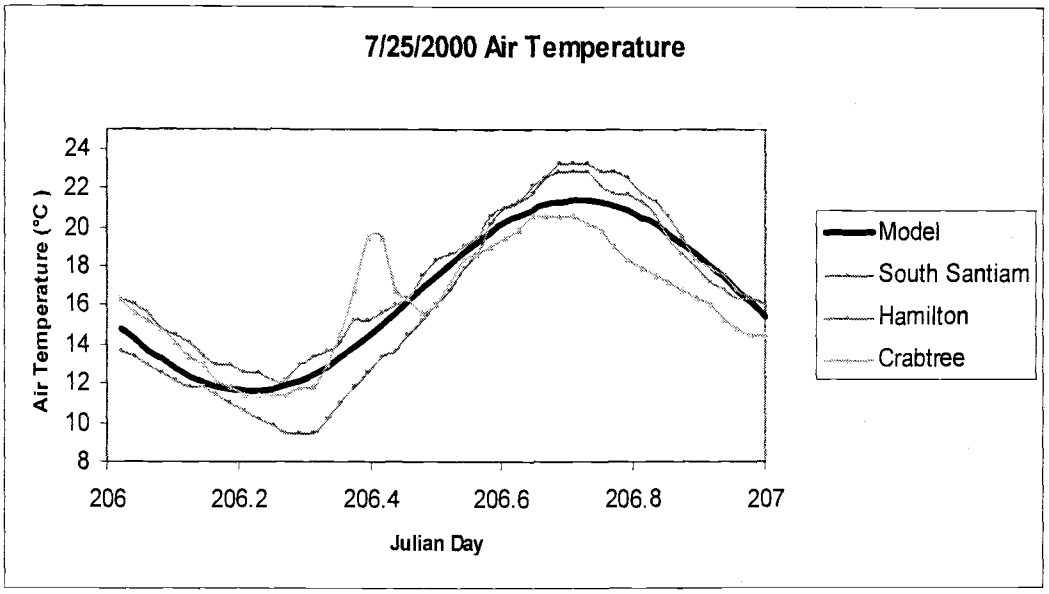

Figure 2A.1 - 7/25/2000 Air Temperature Regression

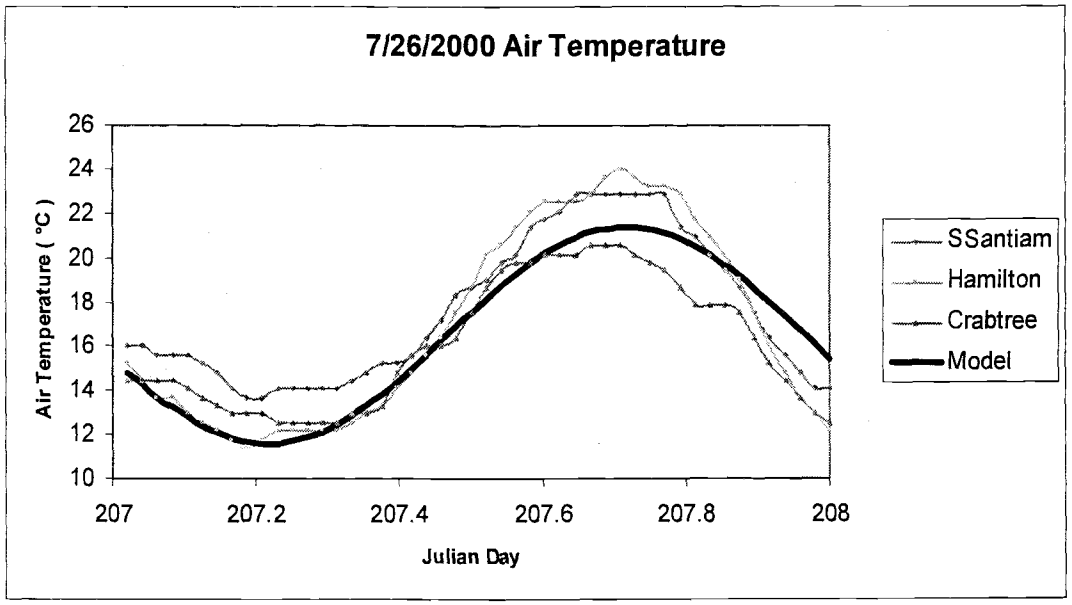

Figure 2A.2 - 7/26/2000 Air Temperature and Sinusoidal Model

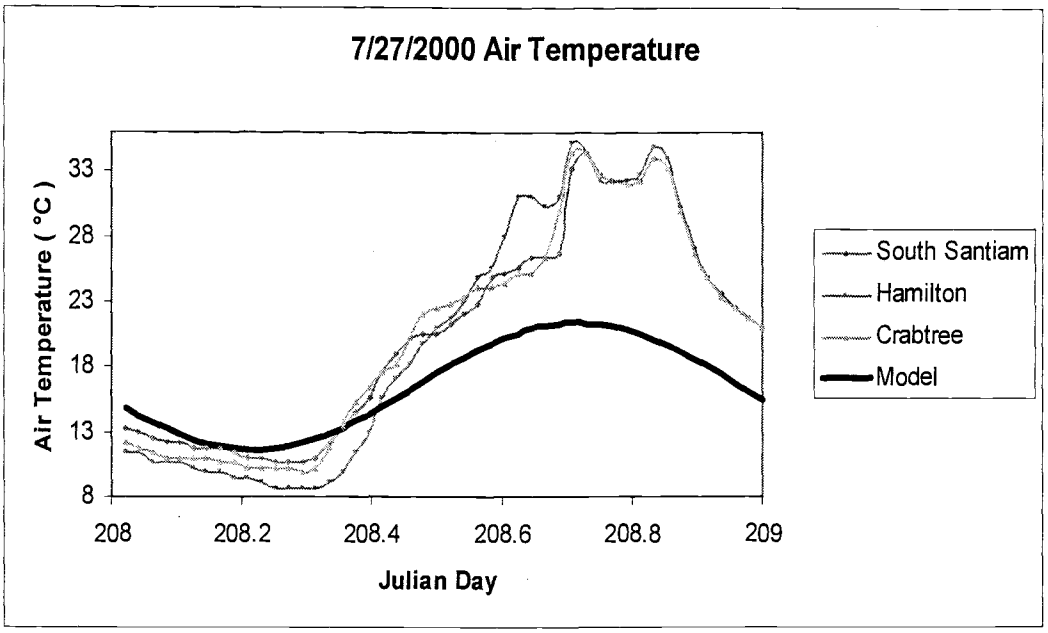

Figure 2A.3 - 7/27/2000 Air Temperature and Sinusoidal Model

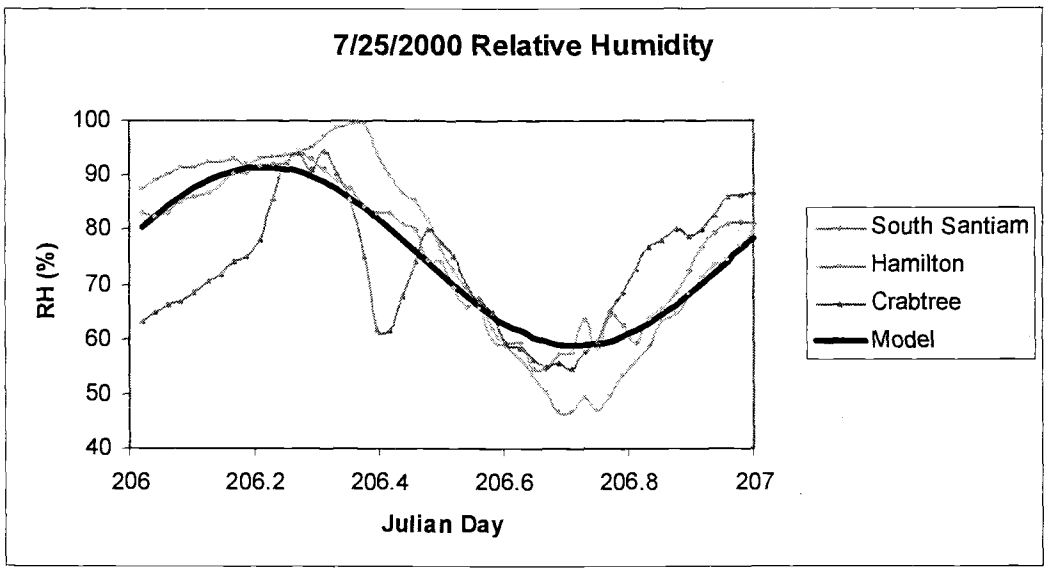

Figure 2A.4 - 7/25/2000 Relative Humidity Regression

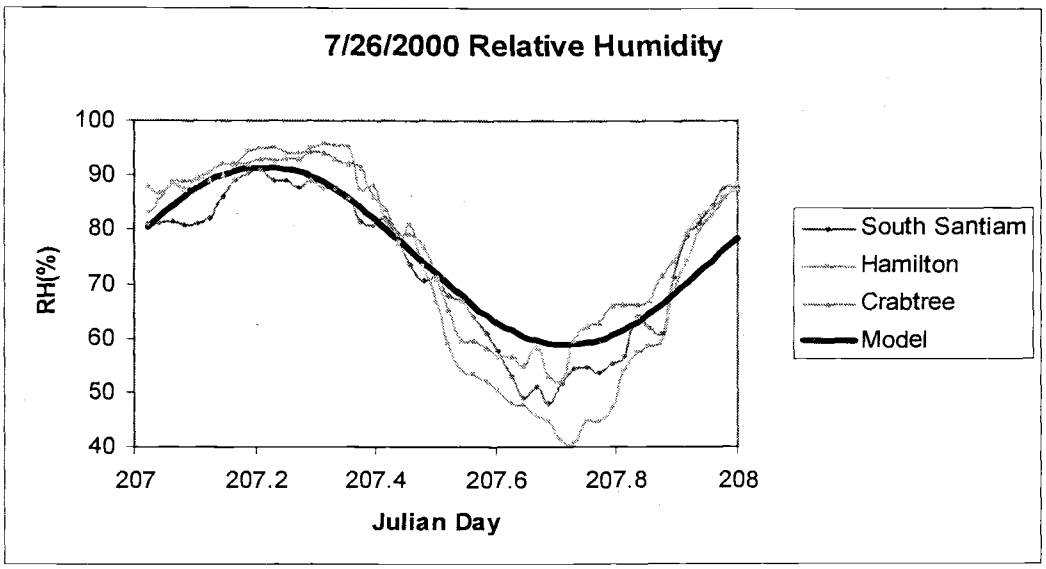

Figure 2A.5 - 7/26/2000 Relative Humidity and Sinusoidal Model

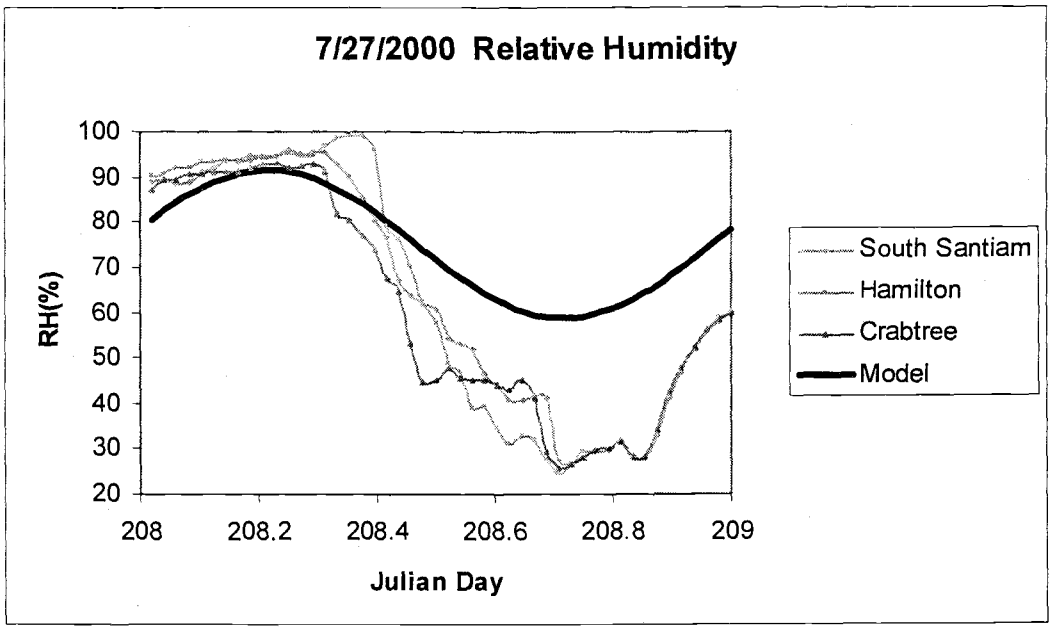

Figure 2A.6 - 7/27/2000 Relative Humidity and Sinusoidal Model

Appendix 2B – Wind Speed

Measured wind speed data from a riparian area was obtained from a site (Sherri L. Johnson, unpublished data) in the HJ Andrews Experimental Forest, a west Oregon Cascades research location. The HJA is located approximately 30 miles south of the South Santiam watershed. This particular data was measured on a second order stream in an alder dominated riparian area. Data was unavailable to the days simulated in this study (July 27th and 28th). August 14 was chosen randomly out of set of 7 days in August. The intent of using measured data from a randomly selected day is to simulate the probable variation of diurnal wind speed fluctuations. Evaporation coefficients are then used as multipliers to adjust the overall magnitude of evaporation flux.

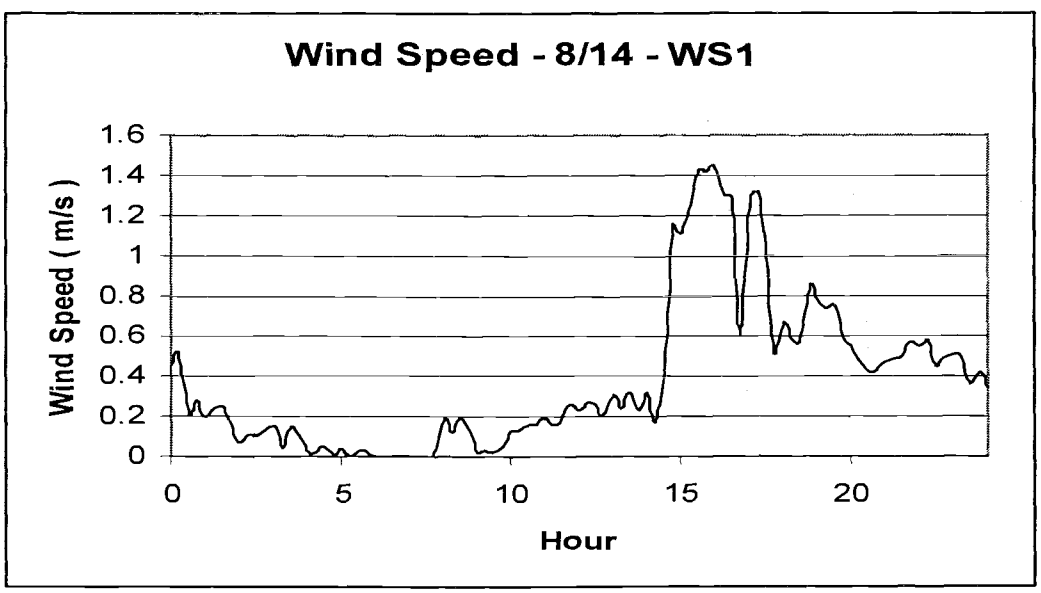

Figure 2B.1 - Forested Riparian Zone Wind Speed Profile

Appendix 2C – Land Use/Land Cover Height and Density Assumptions

Land Use/ Land Cover Class Description	LULC_C ID	VegHeight(m)	VegDensity
Residential 0-4 DU/ac	1	0	0
Residential 4-9 DU/ac	2	0	0
Residential 9-16 DU/ac	3	0	0
Residential 16 DU/ac	4	0	0
Vacant	5	0	0
Commercial	6	0	0
Comm/Industrial	7	0	0
Industrial	8	0	0
Industrial & Comm.	9	0	0
Residential & Comm.	10	0	0
Urban non-vegetated unknown	11	0	0
Civic/open space	12	0	0
Rural structures	16	0	0
2 acre structure influence zone	17	0	0
Railroad	18	0	0
Primary roads	19	0	0
Secondary roads	20	0	0
Light duty roads	21	0	0
Other roads	22	0	0
Rural non-vegetated unknown	24	0	0
Rural Service Center	25	0	0
Built high density	26	0	0
Built medium density	27	0	0
Built low density	28	0	0
Channel non-vegetated	29	0	0
Stream orders. 1-4	31	0	0
Stream orders 5-7	32	0	0
Water	33	0	0
Topo. Shadow	39	0	0
Snow	40	0	0
Barren	42	0	0
Urban tree overstory	49	15	30
Forest open	51	20	15
Forest Semi-closed mixed	52	20	55
Forest Closed hardwood	53	15	80
Forest Closed mixed	54	20	80
Forest Semi-closed conifer	55	35	55

Table 2C.1 Vegetation Height and Density Assumptions (continued)

Land Use/ Land Cover Class Description	LULC_C ID	VegHeight(m)	VegDensity
Forest Closed Conifer 0-20 yr	56	4	85
FCC 21-40 yrs	57	14	85
FCC 41-60 yrs.	58	21.5	85
FCC 61-80 yrs	59	29	85
FCC 81-200 yrs	60	43	85
FCC 200 yrs	61	60	75
Forest Semi-closed hardwood	62	15	55
Hybrid poplar	66	10	80
Grass seed-grain-meadow foam	67	0	0
Irrigated annual rotation	68	0	0
Grains	71	0	0
Nursery	72	0	0
Cranberries & Vineyards	73	0	0
Double cropping	74	0	0
Hops	75	0	0
Mint	76	0	0
Radish seed	77	0	0
Sugar beet seed	78	0	0
Row crop	79	0	0
Grass	80	0	0
Burned grass	81	0	0
Field crop	82	0	0
Hay	83	0	0
Late field crop	84	0	0
Pasture	85	0	0
Natural grassland	86	0	0
Natural shrub	87	4	60
Bare/fallow	88	0	0
Flooded/marsh	89	0	0
Irrigated field crop	90	0	0
Turfgrass/park	91	0	0
Orchard	92	8	35
Christmas trees	93	0	0
Pasture/natural grass/xmas tr	94	0	0
Woodlot	95	15	60
Urban grass-shrub	96	0	0
Hedgerow	97	3	85
Oak savanna	98	15	10
Non-tree wetlands	99	0	0
Prairie	100	0	0

Table 2C.1 - Vegetation Height and Density Assumptions

Appendix 2D – Sensitivity Data

The following charts are values recorded during the sensitivity analysis. Relative and absolute sensitivities reported in Tables 2.3-2.12 were calculated from these data.

	Slope Error Statistics (vs. Mouth)							
	Mile 5.7		McDowell Park					
Parameter Change	Heating	Cooling	Heating	Cooling	ΔTmax	ΔTmin	ΔTimeOfMax(hours)	ΔTimeOfMin(hours)
+50%	0.0031	0.0038	0.0202	0.0151	1.19	0.23	0.37	-0.14
+25%	0.0009	0.0011	0.0058	0.0042	0.62	0.13	0.26	-0.04
base	—	—	—	—	—	—	—	—
-25%	0.0014	0.0017	0.0007	0.0013	-0.71	-0.19	0.05	0.04
-50%	0.0066	0.0097	0.0034	0.0070	-1.46	-0.45	-0.04	-0.03

Table 2D.1 – W/D Ratio Sensitivity (McDowell Creek, Julian Day 208)

	Slope Error Statistics (vs. Mouth)							
	Mile 5.7		McDowell Park					
Parameter Change	Heating	Cooling	Heating	Cooling	ΔTmax	ΔTmin	ΔTimeOfMax(hours)	ΔTimeOfMin(hours)
+500%	0.0134	0.0103	0.0068	0.0097	-1.20	-0.78	-0.12	0.53
+50%	0.0002	0.0001	0.0001	0.0001	-0.13	-0.07	0.07	0.02
base	—	—	—	—	—	—	—	—
-50%	0.0002	0.0001	0.0001	0.0001	0.14	0.07	0.12	-0.09
-90%	0.0006	0.0004	0.0003	0.0004	0.25	0.11	0.14	-0.10

Table 2D.2 – EvapA Sensitivity (McDowell Creek, Julian Day 208)

	Slope Error Statistics (vs. Mouth)							
	Mile 5.7		McDowell Park					
Parameter Change	Heating	Cooling	Heating	Cooling	ΔTmax	ΔTmin	ΔTimeOfMax(hours)	ΔTimeOfMin(hours)
+1000%	0.0011	0.0008	0.0004	0.0007	-0.22	-0.10	-0.05	-0.02
+100%	0.0000	0.0000	0.0000	0.0000	-0.02	-0.01	0.08	0.01
+50%	3E-06	2E-06	1E-06	2E-06	-0.01	-0.005	-0.1	0.009
base	---	---	---	---	---	---	---	---
-50%	0.0000	0.0000	0.0000	0.0000	0.01	0.00	0.10	-0.01
-90%	9E-06	7E-06	4E-06	6E-06	0.02	0.01	0.11	-0.01

Table 2D.3 – EvapB Sensitivity (McDowell Creek, Julian Day 208)

	Slope Error Statistics (vs. Mouth)							
	Mile 5.7		McDowell Park					
Parameter Change	Heating	Cooling	Heating	Cooling	ΔTmax	ΔTmin	ΔTimeOfMax(hours)	ΔTimeOfMin(hours)
+50%	0.0010	0.0010	0.0025	0.0025	2.01	2.01	0.00	0.00
+25%	0.0003	0.0003	0.0006	0.0006	1.01	1.01	0.00	0.00
base	---	---	---	---	---	---	---	---
-25%	0.0003	0.0003	0.0006	0.0006	-1.01	-0.40	0.00	-0.07
-50%	0.0010	0.0010	0.0025	0.0025	-2.01	-1.31	0.01	0.01

Table 2D.4 – $T_{groundwater}$ Sensitivity (McDowell Creek, Julian Day 208)

	Slope Error Statistics							
	Mile 5.7		McDowell Park					
Parameter Change	Heating	Cooling	Heating	Cooling	ΔTmax	ΔTmin	ΔTimeOfMax(hours)	ΔTimeOfMin(hours)
+50%	0.0094	0.0087	0.0062	0.0042	0.13	0.36	0.49	0.06
+25%	0.0041	0.0030	0.0029	0.0014	0.05	0.21	1.02	0.02
base	---	---	---	---	---	---	---	---
-25%	0.0062	0.0039	0.0048	0.0016	-0.03	-0.35	-0.17	-0.11
-50%	0.0265	0.0197	0.0202	0.0091	-0.12	-0.78	-0.59	-0.44

Table 2D.5 – Manning's n Sensitivity (McDowell Creek, Julian Day 208)

	Slope Error Statistics (vs. Mouth)							
	Mile 5.7		McDowell Park					
Parameter Change	Heating	Cooling	Heating	Cooling	ΔTmax	ΔTmin	ΔTimeOfMax(hours)	ΔTimeOfMin(hours)
+400%	0.0078	0.0501	0.0057	0.0284	-2.07	0.13	-3.87	0.24
+100%	0.0005	0.0032	0.0003	0.0017	-0.74	0.04	0.24	0.06
+50%	0.0001	0.0008	8E-05	0.0004	-0.37	0.02	-0.09	0.04
base	---	---	---	---	---	---	---	---
-50%	0.0001	0.0008	0.0001	0.0004	0.37	-0.02	0.09	-0.04
-90%	0.0004	0.0026	0.0003	0.0014	0.68	-0.04	0.07	-0.06

Table 2D.6 – Cloud Fraction Sensitivity (McDowell Creek, Julian Day 208)

	Slope Error Statistics (vs. Mouth)							
	Mile 5.7		McDowell Park					
Parameter Change	Heating	Cooling	Heating	Cooling	ΔTmax	ΔTmin	ΔTimeOfMax(hours)	ΔTimeOfMin(hours)
+50%	0.0068	0.0160	0.0052	0.0073	-0.82	0.36	0.70	0.12
+25%	0.0053	0.0068	0.0041	0.0029	-0.48	0.22	1.26	0.06
base	---	---	---	---	---	---	---	---
-25%	0.0120	0.0086	0.0104	0.0025	0.76	-0.39	-0.33	-0.20
-50%	0.0795	0.0306	0.0559	0.0099	1.76	-0.93	-0.90	-0.68

Table 2D.7 – Volume Multiplier Sensitivity (McDowell Creek, Julian Day 208)

	Slope Error Statistics (vs. Mouth)							
	Mile 5.7		McDowell Park					
Parameter Change	Heating	Cooling	Heating	Cooling	ΔTmax	ΔTmin	ΔTimeOfMax(hours)	ΔTimeOfMin(hours)
+50%	0.0107	0.0075	0.0086	0.0033	-0.05	-0.48	-0.37	-0.20
+25%	0.0040	0.0024	0.0031	0.0010	-0.01	-0.27	-0.19	-0.07
base	---	---	---	---	---	---	---	---
-25%	0.0061	0.0049	0.0043	0.0023	0.08	0.26	1.18	0.05
-50%	0.0137	0.0144	0.0088	0.0054	0.22	0.57	0.37	-0.22

Table 2D.8 – Flow Multiplier Sensitivity (McDowell Creek, Julian Day 208)

	Slope Error Statistics (vs. Mouth)							
	Mile 5.7		McDowell Park					
Parameter Change	Heating	Cooling	Heating	Cooling	ΔTmax	ΔTmin	ΔTimeOfMax(hours)	ΔTimeOfMin(hours)
+50%	0.0028	0.0029	0.0008	0.0008	5.74	5.75	-0.01	-0.01
+25%	0.0007	0.0007	0.0002	0.0002	2.87	2.88	0.00	-0.01
base	—	—	—	—	—	—	—	—
-25%	0.0007	0.0007	0.0002	0.0002	-2.65	-2.12	0.01	0.02
-50%	0.0027	0.0028	0.0007	0.0008	-4.23	-5.02	0.03	0.03

Table 2D.9 – $T_{initial}$ Sensitivity (McDowell Creek, Julian Day 208)

Appendix 2E

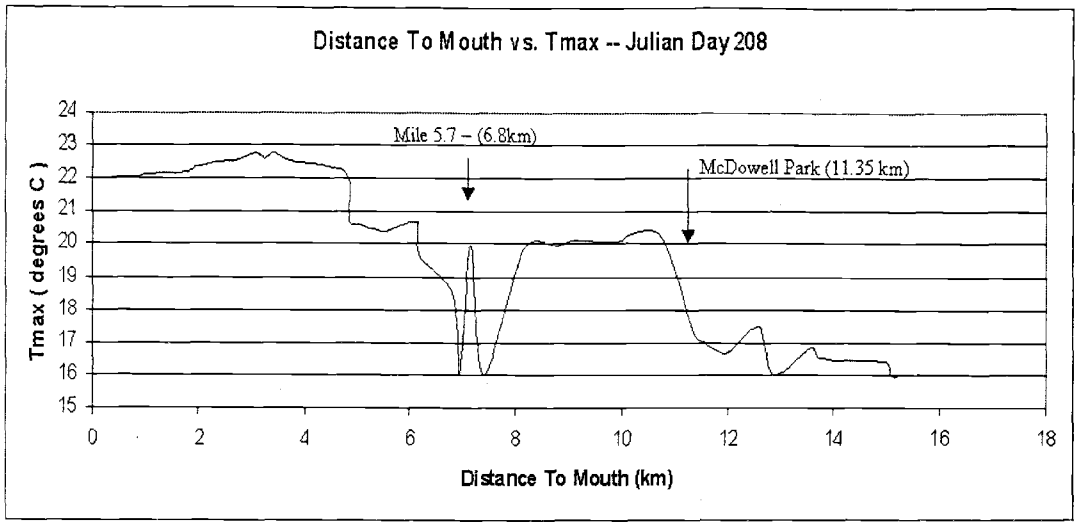

Figure 2E.1 - Temperature Discontinuities at Flow Observations

Conclusions

The development of WET-Temp addresses the lack of a stream temperature model that fully utilizes spatially distributed data. The model represents the stream as a network rather than an aggregation of individual reaches, allowing for dynamic watershed scale analyses than have been impossible previously. WET-Temp utilizes spatially explicit datasets for the calculation of stream temperature responses to land use changes at fine spatial resolutions across the network.

WET-Temp successfully predicted maximum stream temperatures (0.6°C mean difference between measured and modeled) when calibrated to McDowell Creek. It follows that potential changes in riparian vegetation, in the context of stream restoration, can be examined to determine their effect on stream temperature distributions. Maximum stream temperature is a regulatory standard, and WET-Temp should prove useful is studies focused on regulatory concerns.

Examination of temperature distribution across stream networks, as a connective phenomenon as opposed to a reach scale phenomenon, begins to shed light on how networks respond to perturbations in their energetic environment. Many difficulties exist when attempting to model these networks. Adequate descriptions of the physical landscape, especially channel structure and hydrology, need to be addressed more completely. Calibrations within the basin of study are necessary at this point to ensure confidence in the results of analyses within that basin.

WET-Temp does not replace existing reach scale models, but instead is able to answer different questions. The use of WET-Temp in conjunction with reach scale analyses could potentially provide valuable insight into the factors driving observed stream temperature distributions, and provide solid support for the evaluation of management decisions.

Bibliography

Bartholow, J.M. 1995. The stream network temperature model (SNTEMP): A decade of results. Pages 57-60 *in* Ahuja, L., K. Rojas and E. Seely, editors. Workshop on Computer Applications in the Water Management, Proceedings of the 1995 Workshop. Water Resources Research Institute, Fort Collins, Colorado. Information Series No. 79. 292 pp.

Bartholow, J.M. 1990. Stream temperature model. Pages IV-20 to IV-47 in W.S. Platts ed. Managing Fisheries and Wildlife on Rangelands grazed by Livestock: A guidance and reference document for biologists. W.S. Platts and Assoc. for the Nevada Department of Wildlife. December, 1990. v.p.

Belksy, A.J., A. Matzke and S.Uselman. 1999. Survey of livestock influences on stream and riparian ecosystems in the western United States. Journal of Soil and Water Conservation 54(1) : 419-431.

Beschta, R.L. and J. Weatherred. 1984. A computer model for predicting stream temperatures resulting from the management of streamside vegetation. *USDA Forest Service.* WSDG-AD-00009.

Beschta, R.L., R.E. Bilby, G.W. Brown, L.B. Holtby and T.D. Hofstra, 1987. Stream Temperature and Aquatic Habitat : Fisheries and Forestry Interactions. *In* Streamside Management : Forestry and Fisheries Interactions, E.O. Salo and T.W. Cundy (Editors). Contribution No. 57, University of Washington, Institute of Forest Resources, 471 pp.

Beschta, R.L. 1997. Riparian Shade and Stream Temperature: An Alternative Perspective. *Rangelands* 19(2): 25-28.

Bowie, G.L., Mills, W.B., Porcella, D.B., Campbell, C.L., Pagenkopf, J.R., Rupp, G.L., Johnson, K.M., Chan, P.W., and S.A. Gherini. 1985. Rates, Constants, and Kinetics Formulations in Surface Quality Modelling, 2nd Edition. EPA/600/3-85/040, U.S. Environmental Protection Agency, Athens, GA.

Boyd, M. 1996. Heat Source : Stream, River and Open Channel Temperature Prediction. Master's thesis. Oregon State University, Corvallis, OR.

Brown, George W. 1969. Predicting Temperatures of Small Streams. Water Resources Research. 5(1) : 68-75.

Brown G.W. and J.T. Krygier. 1970. Effects of Clear-Cutting on Stream Temperatures. Water Resources Research 6(4) : 1133-1140.

Brunke, M., and T. Gonser. The ecological significance of exchange processes between rivers and groundwater. Freshwater Biology. 37 : 1-33.

Carnahan B, Luther, H.A., Wilkes, J.O. 1969. Applied Numerical Methods. John Wiley and Sons, New York, 603pp.

Chen, Y.D. 1996. Hydrologic and water quality modeling for aquatic ecosystem protection and restoration in forest watersheds: a case study of stream temperature in the Upper Grande Ronde River, Oregon. PhD dissertation, University of Georgia, Athens, Ga.

Chen, Y.D., R.F. Carsel, S.C. McCutcheon, and W.L. Nutter. 1998. Stream Temperature Simulation of Forested Riparian Areas: I. Watershed-Scale Model Development. Journal of Environmental Engineering 124(4) : 304-315.

Chen, Y.D., S.C. McCutcheon, D.J. Norton and W.L. Nutter. 1998. Stream Temperature Simulation of Forested Riparian Areas : II. Model Application. Journal of Environmental Engineering 124(4) : 316-328.

Cox, M.M. 2002. A spatially-distributed network-based model for estimating stream temperature distribution. Master's Thesis, Oregon State University, Corvallis, OR.

Chanson, H. 1999. The Hydraulics of Open Channel Flow. Arnold, London, 495pp.

Dingman, S.L. 1994. Physical Hydrology. Prentice Hall, New Jersey, 556pp.

Hauer F.R. and G.A. Lamberti. 1996. Methods in Stream Ecology. Academic Press, San Diego, 674pp.

Horne, A.J. and C.R. Goldman. 1994. Limnology, 2nd edition. McGraw-Hill Inc., New York, 575pp.

Hsieh, J. 1986. Solar Energy Engineering. Prentice Hall Inc., New Jersey, 553pp.

Iqbal, M. 1983. An introduction to solar radiation. Academic Press, Toronto, 390pp.

Jones, H.G. 1983. Plants and Microclimate. A quantitative approach to environmental plant physiology. Cambridge University Press, Cambridge, 323pp.

LeBlanc, R.T., R.D. Brown, and J.E. FitzGibbon. 1997. Modeling the effects of land use change on the water temperature in unregulated urban streams. Journal of Environmental Management 49(4) : 445-469.

McCuthceon, S.C. 1989. Water Quality Modelling: Vol. 1, Transport and Surface Exchange in Rivers. CRC Press, Boca Raton, 334 pp.

McIntosh, B.A. 1992. Historical changes in anadromous fish habitat in the Upper Grande Ronde River, Oregon, 1941-1990. MS Thesis, Oregon State University, Corvallis, OR.

National Marine Fisheries Service. Feb 2, 2000. Northwest Region Species List (Endangered, Threatened, Proposed, and Candidate Species under National Marine Fisheries Service Jurisdiction that Occur in Oregon, Washington, and Idaho). Retrieved March 11, 2002 from http://www.nwr.noaa.gov/1habcon/habweb/listnwr.htm.

Natural Resources Conservation Service. June 13.2001. Soil Survey Geographic (SSURGO) Database. Retrieved March 22, 2002 from http://www.ftw.nrcs.usda.gov/ssurgo.html.

Nehlsen W., Williams, J.E. and J.A. Lichatowich. 1991. Pacific Salmon at the Crossroads: Stocks at Risk from California, Oregon, Idaho and Washington. *Fisheries* 16(2): 4-19.

Northwest Power Planning Council (NPPC). 1992. Strategy for salmon, volumes I and II. Portland, OR.

Oetter, D. R., Cohen, W. B., Berterretche, M., Maiersperger, T. K., and R.E Kennedy. 2001. Land cover mapping in an agricultural setting using multi-seasonal Thematic Mapper data. *Remote Sensing of Environment* 76(2): 139-155.

Oregon Department of Environment Quality. 1998. Oregon DEQ 303(d) list of water quality limited streams and stream segments – Streams Summary Report. Retrieved March 11, 2002 from htttp://www.deq.state.or.us/wq/303dlist/StreamsSummaryReport.htm

Oregon Department of Environmental Quality. 2001. Upper Klamath Lake Drainage Total Maximum Daily Load (TMDL). Draft report.

Oregon Climate Service. 1990. Zone 2 Climate Data Archives – Foster Dam – Monthly means and extremes (1961-1990). Retrieved on March 26, 2002 from http://www.ocs.orst.edu/pub_ftp/climate_data/mme/mme3047.html.

Oregon State University Biosystems Analysis Group. Oct 1, 1998. Developing Methods and Tools for Watershed Restoration – Design , Implementation, and Assessment in the Willamette Basin, Oregon. Retrieved March 24, 2002 from http://biosys.bre.orst.edu/restore/default.cfm.

Oregon Watershed Enhancement Board. Oct 1, 2000. An Overview of Oregon Watershed Councils. Retrieved March 23, 2002 from http://www.oweb.state.or.us/groups/councils.shtml.

Ritchey, D. 2000. Design and Prioritized Implementation of Woody Riparian Buffers for Increasing Effective Shade in Agricultural Landscapes of the Willamette River Valley, Oregon. Masters Project. University of Oregon, Eugene, OR.

Rosgen, D. 1996. Applied River Morphology. Wildland Hydrology, Pagosa Springs, CO.

Schroeter, H.O., D.J. Van Vliet, K. Boehmer and D. Beach. 1996. Continuous in-stream temperature modeling: Integration with a physically based subwatershed hydrology model. Advances in Modeling the Management of Stormwater Impacts., Ann Arbor Press, Inc. Chelsea, MI, pp. 27-48.

Sellars, W.D. 1965. Physical Climatology. University of Chicago Press, Chicago. 272 pp.

Sinokrot, B.A. and H.G. Stefan. 1993. Stream Temperature Dynamics : Measurements and Modeling. Water Resources Research. 29(7) : 2299-2312.

South Santiam Waterhsed Council and E&S Environmental Chemistry Inc. 1999. South Santiam Watershed Assessment. Draft Final Report.

Sullivan, K. and T.N. Adams. 1991. The Physics of Stream Heating: 2) An analysis of temperature patterns in stream environments based on physical principles and field data. Weyerhaeuser Technical Report 044 -5002/89/2.

Theurer, F.D., K.A. Voos, and W.J. Miller. 1984. Instream Water Temperature Model. Instream Flow Information Paper 16. *U.S. Fish and Wildlife Service.* FWS/OBS-84/15. 200 pp.

Togersen, C.E., D.M. Price, H.W. Li, and B.A. McIntosh. Multiscale Thermal Refugia and Stream Habitat Associations of Chinook Salmon in Northeastern Oregon. *Ecological Applications*, 9(1): 301-319.

Wilson, W.J., M.D. Kelley, and P.R. Meyer. 1987. Instream temperature modeling and fish impact assessment for a proposed large-scale Alaska hydroelectric project. Pages 183-206 *in* J.F. Craig and J.B. Kemper, eds. Regulated streams. Plenum Press, New York, 431 pp.